

# Statistical mechanics of two-dimensional Euler flows and minimum enstrophy states

A. Naso, P.H. Chavanis and B. Dubrulle

<sup>1</sup> Laboratoire de Physique, Ecole Normale Supérieure de Lyon and CNRS (UMR 5672), 46 allée d'Italie, 69007 Lyon, France

<sup>2</sup> Laboratoire de Physique Théorique (IRSAMC), CNRS and UPS, Université de Toulouse, F-31062 Toulouse, France

<sup>3</sup> SPEC/IRAMIS/CEA Saclay, and CNRS (URA 2464), 91191 Gif-sur-Yvette Cedex, France

e-mail: aurore.naso@ens-lyon.fr, chavanis@irsamc.ups-tlse.fr, berengere.dubrulle@cea.fr

To be included later

**Abstract.** A simplified thermodynamic approach of the incompressible 2D Euler equation is considered based on the conservation of energy, circulation and microscopic enstrophy. Statistical equilibrium states are obtained by maximizing the Miller-Robert-Sommeria (MRS) entropy under these sole constraints. We assume that these constraints are selected by properties of forcing and dissipation. We find that the vorticity fluctuations are Gaussian while the mean flow is characterized by a linear  $\bar{\omega} - \psi$  relationship. Furthermore, we prove that the maximization of entropy at fixed energy, circulation and microscopic enstrophy is equivalent to the minimization of macroscopic enstrophy at fixed energy and circulation. This provides a justification of the minimum enstrophy principle from statistical mechanics when only the microscopic enstrophy is conserved among the infinite class of Casimir constraints. A new class of relaxation equations towards the statistical equilibrium state is derived. These equations can serve as numerical algorithms to determine maximum entropy or minimum enstrophy states. We use these relaxation equations to study geometry induced phase transitions in rectangular domains. In particular, we illustrate with the relaxation equations the transition between monopoles and dipoles predicted by Chavanis & Sommeria [J. Fluid. Mech. **314**, 267 (1996)]. We take into account stable as well as metastable states and show that metastable states are robust and have negative specific heats. This is the first evidence of negative specific heats in that context. We also argue that saddle points of entropy can be long-lived and play a role in the dynamics because the system may not spontaneously generate the perturbations that destabilize them.

**PACS.** 0 5.20.-y Classical statistical mechanics - 05.45.-a Nonlinear dynamics and chaos - 05.90.+m Other topics in statistical physics, thermodynamics, and nonlinear dynamical systems - 47.10.-g General theory in fluid dynamics - 47.15.ki Inviscid flows with vorticity - 47.20.-k Flow instabilities - 47.32.-y Vortex dynamics; rotating fluids

## 1 Introduction

Two-dimensional turbulence has the striking property of organizing spontaneously into large-scale coherent structures. These coherent structures correspond to jets and vortices in geophysical and astrophysical flows [1, 2]. They can be reproduced in numerical simulations [3] and laboratory experiments [4, 5] in either forced or unforced situations. These coherent structures involve the presence of a mean flow and fluctuations around it. The mean flow turns out to be a steady state of the pure 2D Euler equations (without forcing and dissipation) at some coarse-grained scale. In several cases, the steady state is characterized by a linear relationship between vorticity  $\omega$  (or potential vorticity  $q = \omega + h$  in the presence of a topography  $h$ ) and stream function  $\psi$ . For example, the case of a linear  $q - \psi$  relationship was considered early by Fofonoff (1954) [6] as a simple model of oceanic circulation. These

“Fofonoff flows” were found to emerge naturally from random initial conditions in numerical experiments of forced and unforced 2D turbulence [7, 8, 9, 10, 11]. However, these results are not expected to be general. There exists many other cases in 2D turbulence where the  $q - \psi$  relationship is not linear. The understanding and prediction of these quasi stationary states (QSS), in forced and unforced situations, is still a challenging problem. Different approaches have been proposed to describe these QSSs.

In the case of forced flows (for example oceanic flows experiencing a forcing by the wind and a dissipation), Nilner (1966) [12] and Marshall & Nurser (1986) [13] have proposed that forcing and dissipation could equilibrate each other in average and determine a QSS that is a steady state of the unforced and inviscid 2D Euler equation. This QSS is characterized by a functional relationship  $q = f(\psi)$  between potential vorticity and stream function where the

function  $f$  is selected by the properties of forcing and dissipation. In particular, these authors discussed the properties that forcing must possess to generate Fofonoff flows.

In the case of unforced flows, a phenomenological approach, called the minimum enstrophy principle, was proposed by Bretherton & Haidvogel (1976) [14]. It is based on the inverse cascade<sup>1</sup> process of Batchelor (1969) [15]. It is argued that, in the presence of a small viscosity, the (potential) enstrophy decays while the energy is approximately conserved. This is what Matthaeus & Montgomery (1980) [16] have called selective decay. In that case, we can expect that the system will relax towards a state that minimizes (potential) enstrophy at fixed energy. This is mainly a postulate. This principle leads to a steady state of the 2D Euler equation characterized by a linear  $q - \psi$  relationship. When applied to geophysical flows, this principle can give an alternative justification of Fofonoff flows. The minimum enstrophy principle has been generalized by Leith (1984) [17] so as to take into account the conservation of angular momentum in order to describe isolated vortices. However, this principle is purely phenomenological and it is difficult to establish its domain of validity.

A statistical mechanics approach of 2D turbulence has been developed by Kraichnan (1967,1975) [18,19] based on the truncated Euler equations. In that case, the dynamics conserves only the energy and the enstrophy (the other constraints of the Euler equation are lost by the truncation). Since this system is Liouvillian, we can apply the methods of statistical mechanics. This is the so-called energy-enstrophy statistical theory. In the absence of topography, the truncated statistical mechanics predicts a homogeneous flow with an equilibrium energy spectrum of the form  $E(k) = k/(a + bk^2)$  corresponding to an equipartition distribution. In the presence of a topography (or  $\beta$ -effect), this statistical mechanics approach was generalized by Salmon, Holloway & Hendershott (1976) [20]. It leads to a mean flow where the average potential vorticity  $q$  and the average stream function  $\psi$  are related to each other by a linear relationship. When applied to geophysical flows, this approach provides a justification of Fofonoff flows from statistical mechanics. However, the fact that the truncated statistical mechanics breaks the conservation of some integrals of the 2D Euler equations may be considered as a limitation of this approach.

Another statistical mechanics of 2D turbulence, based on a point vortex approximation, was initiated by Onsager (1949) [21] and further developed by Joyce & Montgomery (1973) [22] and Lundgren & Pointin (1977) [23] in a mean field approximation. The statistical equilibrium state maximizes the usual Boltzmann entropy (adapted to point vortices) while conserving the energy and the number of vortices of each species. This statistical mechanics predicts an equilibrium state where the relationship between vorticity

and stream function is given by a Boltzmann distribution, or a superposition of Boltzmann distributions (on the different species). However, the point vortex approximation is a crude approximation of real turbulent flows where the vorticity field is continuous.

A statistical theory of 2D turbulence valid for continuous vorticity fields has been developed by Miller (1990) [24] and Robert & Sommeria (1991) [25]. This theory takes into account all the constraints of the 2D Euler equation. The statistical equilibrium state maximizes a mixing entropy while conserving energy, circulation and all the Casimirs. This leads to equilibrium states with more general mean flows than in the previous approaches. In particular, the  $\bar{\omega} - \psi$  relationship and the fluctuations around it are determined by the initial conditions and can take various shapes. However, some connections with the earlier works can be found. For example, Robert & Sommeria (1991) [25] note that the results of the point vortex approach can be recovered in the dilute limit of their statistical theory. On the other hand, Miller (1990) [24] notes that for specific initial conditions leading to a Gaussian vorticity distribution at statistical equilibrium, the mean flow has a linear  $\bar{\omega} - \psi$  relationship similar to that obtained from the minimum enstrophy principle. Finally, Chavanis & Sommeria (1996) [26] consider a limit of strong mixing (or low energy) of the MRS theory in which  $\beta\psi \ll 1$  and find some connections between maximum entropy states and minimum enstrophy states. In that limit, the maximization of entropy at fixed energy, circulation and Casimirs becomes equivalent to the minimization of the macroscopic enstrophy  $\Gamma_2^{c,g} = \int \bar{\omega}^2 d\mathbf{r}$  at fixed energy and circulation. This justifies a form of inviscid minimum enstrophy principle in a well-defined limit of the statistical theory<sup>2</sup>. This strong mixing limit also makes a hierarchy among the Casimir constraints. To lowest order in the expansion  $\beta\psi \ll 1$ , leading to a linear  $\bar{\omega} - \psi$  relationship, only the circulation  $\Gamma$  and the microscopic enstrophy  $\Gamma_2^{f,g} = \int \bar{\omega}^2 d\mathbf{r}$  are important. To next orders, leading to nonlinear  $\bar{\omega} - \psi$  relationships, higher and higher moments  $\Gamma_n^{f,g} = \int \bar{\omega}^n d\mathbf{r}$  become relevant.

Recently, an alternative statistical theory has been proposed by Ellis, Haven & Turkington (2002) [29] and further discussed by Chavanis (2005,2008) [30,31]. These authors argue that, in real situations where the flows are forced and dissipated at small scales, the conservation of all the constraints of the 2D Euler equation is abusive. They propose to keep only the robust constraints (energy and circulation) and treat the fragile constraints canonically. This amounts to prescribing a prior vorticity distribution instead of the Casimirs. This can be viewed as a grand microcanonical version of the Miller-Robert-Sommeria (MRS) theory. In the Ellis-Haven-Turkington (EHT) approach, the statistical equilibrium state maxi-

<sup>1</sup> In 3D turbulence, energy cascades towards smaller and smaller scales where it is dissipated by viscosity. In 2D turbulence, the energy is transferred to larger and larger distances in an inverse cascade (explaining its conservation) whereas this is the enstrophy that is transferred to shorter and shorter scales, and dissipated.

<sup>2</sup> In a different situation, Brands *et al.* (1999) [27] show that, in case of incomplete relaxation, the statistical equilibrium state restricted to a “maximum entropy bubble” because of lack of ergodicity [28] can resemble a minimum enstrophy state. However, this agreement is rather fortuitous and is not expected to be general.

mizes a relative entropy (determined by the prior) while conserving energy and circulation. The mean flow turns out to maximize a generalized entropy determined by the prior at fixed circulation and energy. For a Gaussian prior, the generalized entropy is proportional to minus the macroscopic enstrophy. This justifies a minimum enstrophy principle from statistical mechanics when the constraints are treated canonically and the prior is Gaussian. Furthermore, this approach allows to go beyond the minimum enstrophy principle by considering more complicated priors.

We can give another interpretation of the EHT approach. Indeed, Bouchet (2008) [32] notes that the EHT approach provides a *sufficient* condition of MRS stability. Indeed, it is well-known in statistical mechanics and optimization theory [33] that a solution of a maximization problem is always a solution of a more constrained dual maximization problem. Thus, grand microcanonical stability (EHT) implies microcanonical stability (MRS). Therefore, if the mean flow maximizes a generalized entropy at fixed circulation and energy, then the corresponding Gibbs state is a MRS equilibrium state. However, the reciprocal is wrong in case of ensemble inequivalence (between microcanonical and grand microcanonical ensembles) that is generic for systems with long-range interactions [33]. The mean flow associated to a MRS equilibrium state does not necessarily maximize a generalized entropy at fixed circulation and energy. In this sense, the minimization of enstrophy at fixed circulation and energy provides a sufficient, but not necessary, condition of MRS stability. A review of the connections between these different variational principles has been given recently by Chavanis (2009) [34].

In this paper, we shall complement these different approaches by considering a sort of intermediate situation between all these theories. We argue that, in most physical situations, the system is forced and dissipated at small scales. In some situations, forcing and dissipation equilibrate each other so that the system becomes, in average, statistically equivalent to the 2D Euler equation where forcing and dissipation are “switched-off”. In particular, a quasi stationary state (QSS) can form on a relatively short timescale. This QSS involves a mean flow and fluctuations around it. We propose to describe this state in terms of the statistical mechanics of the 2D Euler equation. However, we indirectly take into account the effects of forcing and dissipation in the choice of the constraints. The energy and the circulation must be obviously conserved. By contrast, the conservation of all the Casimir invariants is abusive and it is likely that some Casimir invariants will be destroyed by the forcing and the dissipation. We argue that some Casimir invariants are more relevant than others and that they will be selected by the properties of forcing and dissipation. In that case, the statistical equilibrium state is expected to maximize the MRS entropy with these sole constraints. It is not our goal here to determine how these constraints are selected by the properties of forcing and dissipation. This is clearly a complicated problem that has to be tackled by other methods. We shall just use a

heuristic approach and consider the situation where these relevant constraints are the circulation, the energy and the microscopic enstrophy. In other words, among all the Casimir constraints, we only consider the quadratic one. We do not claim that this is the most general situation but simply that it is a case of physical interest. We therefore consider *the maximization of the MRS entropy at fixed circulation, energy and microscopic enstrophy* and provide a detailed study of this (non trivial) variational principle. Our maximization principle is similar in spirit to the approach of Kraichnan, which only considers the conservation of energy and enstrophy, except that we remain in physical space and work with the MRS entropy for the distribution of vorticity levels while Kraichnan works in Fourier space.

It may be noted that our approach is partly motivated by results of experiments carried out in von Karman flows [35,36]. In fact, the present paper, valid for the 2D Euler equations, prepares the ground before considering the more complicated (but similar) case of 3D axisymmetric turbulence treated in [37]. In that later case, we show the equivalence between maximum entropy states at fixed helicity, angular momentum and microscopic energy and minimum macroscopic energy states at fixed helicity and angular momentum. Therefore, our two approaches are closely related and provide a statistical basis for justifying the phenomenological minimum enstrophy (2D) and minimum energy (3D axisymmetric) principles [16].

The paper is organized as follows.

In Sec. 2, we discuss some general properties of the steady states of the 2D Euler equations. In particular, we mention the refined criterion of nonlinear dynamical stability given by Ellis *et al.* [29] based on the maximization of a pseudo entropy at fixed circulation and energy.

In Sec. 3, we recall the phenomenological minimum entropy principle based on selective viscous decay.

In Sec. 4, we discuss the connection between maximum entropy states and minimum enstrophy states. In Sec. 4.1, we consider the maximization of the MRS entropy at fixed energy, circulation and microscopic enstrophy (energy-entropy statistical mechanics). This maximization problem leads to a statistical equilibrium state with Gaussian fluctuations and a mean flow characterized by a linear  $\bar{\omega} - \psi$  relationship. In Sec. 4.2, we introduce an equivalent, but simpler, maximization problem based on the maximization of an entropic functional of the coarse-grained vorticity at fixed circulation, energy and microscopic enstrophy. This generalized entropy has some similarities with the Renyi entropy [38,39]. In Sec. 4.3, we show *the equivalence between the maximization of entropy at fixed energy, circulation and microscopic enstrophy and the minimization of macroscopic enstrophy at fixed energy and circulation*<sup>3</sup>. Therefore, our simplified

<sup>3</sup> This equivalence is not trivial. For example, in the MRS approach where all the Casimirs are conserved, there exists particular initial conditions leading to a Gaussian Gibbs state at equilibrium associated with a linear  $\bar{\omega} - \psi$  relationship [24]. However, we cannot conclude that these states are minimum enstrophy states (they could be just saddle points of enstro-

thermodynamic approach provides a justification of the minimum enstrophy principle (and Fofonoff flows) from statistical mechanics when only the microscopic enstrophy is conserved among the infinite class of Casimir constraints.

We also derive relaxation equations associated with the various maximization problems mentioned above (for the reader's convenience, the formal derivation of these relaxation equations is postponed to Appendix D). Associated with the basic variational problem, we derive a relaxation equation for the vorticity distribution that increases the MRS entropy at fixed energy, circulation and microscopic enstrophy. In that case, the vorticity distribution  $\rho(\mathbf{r}, \sigma, t)$  progressively becomes Gaussian and the mean flow  $\bar{\omega}(\mathbf{r}, t)$  relaxes towards a steady state characterized by a linear  $\bar{\omega} - \psi$  relationship. Associated with the simplified variational problem, we derive a relaxation equation for the mean flow that increases a generalized entropy (Renyi-like) while conserving energy, circulation and microscopic enstrophy. In that case, the vorticity distribution is always Gaussian, even in the out-of-equilibrium regime, with a uniform centered variance monotonically increasing with time. Associated with the minimum enstrophy principle, we derive a relaxation equation for the mean flow that dissipates the macroscopic enstrophy while conserving energy and circulation. These relaxation equations can serve as numerical algorithms to determine maximum entropy or minimum enstrophy states with appropriate constraints.

In Sec. 5, we study minimum enstrophy states at fixed energy and circulation in rectangular domains. This problem was first considered by Chavanis & Sommeria (1996) [26] who report interesting phase transitions between monopoles and dipoles depending on the geometry of the domain (e.g., the aspect ratio  $\tau$  of a rectangular domain) and on the value of the control parameter  $\Gamma^2/E$ . In particular, for  $\Gamma = 0$ , they report a transition from a monopole to a dipole when the aspect ratio becomes larger than  $\tau_c = 1.12$ . For  $\Gamma \neq 0$  and  $\tau < \tau_c$ , the maximum entropy state is always a monopole and for  $\Gamma \neq 0$  and  $\tau > \tau_c$ , the maximum entropy state is a dipole for small  $\Gamma^2/E$  and a monopole for large  $\Gamma^2/E$ . They also studied the metastability of the solutions (local entropy maxima) and the possible transition between a direct and a reversed monopole. This work has been followed recently in different directions. Venaille & Bouchet (2009) [40] have investigated in detail the nature of these phase transitions

phy at fixed circulation and energy). We can only prove that a minimum of enstrophy (more generally a maximum of a “generalized entropy”) at fixed circulation and energy is MRS thermodynamically stable [32,34] but this is not reciprocal: the coarse-grained vorticity field associated with a MRS equilibrium state is not necessarily a minimum of enstrophy (or more generally a maximum of a “generalized entropy”) at fixed circulation and energy. By contrast, if we keep only the microscopic enstrophy as a constraint among all the Casimirs, we shall prove here that the Gibbs state is a maximum entropy state at fixed circulation, microscopic enstrophy and energy iff the corresponding coarse-grained vorticity field is a minimum of macroscopic enstrophy state at fixed circulation and energy.

from the viewpoint of statistical mechanics. In particular, they showed that the point ( $\Gamma = 0, \tau_c = 1.12$ ) corresponds to a bicritical point separating a microcanonical first order transition line to two second order transition lines. Keetels, Clercx & van Heijst (2009) [41] have studied minimum enstrophy states in rectangular or circular domains with boundary conditions taking into account the effect of viscosity. Finally, Taylor, Borchardt & Helander (2009) [42] have shown that the two types of solutions appearing in the study of Chavanis & Sommeria [26] could explain the process of “spin-up” discovered by Clercx, Maassen & van Heijst (1998) [43]. In Sec. 5, we recall and complete the main results of the approach of Chavanis & Sommeria [26] in order to facilitate the discussion of the last section.

In Sec. 6, we use the relaxation equations derived in Appendix D to illustrate the phase transitions described in Sec. 5. On the basis of the relaxation equations, we observe a persistence of unstable states that are saddle points of entropy. Therefore, we argue that unstable saddle points of entropy may play a role in the dynamics if the system does not spontaneously generate the perturbations that can destabilize them. We also follow an hysteretic cycle as a function of the circulation where the hysteresis is due to the robustness of metastable states (local entropy maxima). Finally, we briefly describe the possibility of transitions between direct and reversed monopoles in the presence of stochastic forcing.

Throughout this paper, we consider the simple case of incompressible 2D flows without topography. However, the main formalism of the theory can be generalized straightforwardly to account for a topography (or a  $\beta$ -effect) by simply replacing the vorticity  $\omega$  by the potential vorticity  $q = \omega + h$ . Some applications will be considered in a companion paper [44]. We also assume throughout the paper that the domain is of unit area  $A = 1$ .

## 2 Dynamical stability of steady states of the 2D Euler equation

We consider a two-dimensional incompressible and inviscid flow described by the 2D Euler equations

$$\frac{\partial \omega}{\partial t} + \mathbf{u} \cdot \nabla \omega = 0, \quad -\Delta \psi = \omega, \quad (1)$$

where  $\omega \mathbf{z} = \nabla \times \mathbf{u}$  is the vorticity,  $\psi$  the stream function and  $\mathbf{u}$  the velocity field ( $\mathbf{z}$  is a unit vector normal to the flow). The 2D Euler equation admits an infinite number of steady states of the form

$$\omega = f(\psi), \quad (2)$$

where  $f$  is an arbitrary function. They are obtained by solving the differential equation

$$-\Delta \psi = f(\psi), \quad (3)$$

with  $\psi = 0$  on the domain boundary.

To determine the dynamical stability of such flows, we can make use of the conservation laws of the 2D Euler



equations. The 2D Euler equations conserve an infinite number of integral constraints that are the energy

$$E = \int \frac{\mathbf{u}^2}{2} d\mathbf{r} = \frac{1}{2} \int \omega \psi d\mathbf{r}, \quad (4)$$

and the Casimirs

$$I_h = \int h(\omega) d\mathbf{r}, \quad (5)$$

where  $h$  is an arbitrary function. In particular, all the moments of the vorticity  $\Gamma_n = \int \omega^n d\mathbf{r}$  are conserved. The first moment  $\Gamma = \int \omega d\mathbf{r}$  is the circulation and the second moment  $\Gamma_2 = \int \omega^2 d\mathbf{r}$  is the enstrophy. Let us consider a special class of Casimirs of the form

$$S = - \int C(\omega) d\mathbf{r}, \quad (6)$$

where  $C$  is a convex function (i.e.  $C'' \geq 0$ ). These functionals are called pseudo entropy [34]. Ellis *et al.* [33] have shown that the maximization problem

$$\max_{\omega} \{S[\omega] \mid E[\omega] = E, \Gamma[\omega] = \Gamma\}, \quad (7)$$

determines a steady state of the 2D Euler equation that is nonlinearly dynamically stable. This provides a refined criterion of nonlinear dynamical stability. The critical points of (7) are given by the variational principle

$$\delta S - \beta \delta E - \alpha \delta \Gamma = 0, \quad (8)$$

where  $\beta$  and  $\alpha$  are Lagrange multipliers. This gives

$$C'(\omega) = -\beta\psi - \alpha \Rightarrow \omega = F(\beta\psi + \alpha), \quad (9)$$

where  $F(x) = (C')^{-1}(-x)$ . We note that  $\omega'(\psi) = -\beta/C''(\omega)$  so that  $\omega(\psi)$  is a monotonic function increasing for  $\beta < 0$  and decreasing for  $\beta > 0$ . This critical point is a steady state of the 2D Euler equation. On the other hand, it is a (local) maximum of the pseudo entropy at fixed energy and circulation iff

$$-\frac{1}{2} \int C''(\omega)(\delta\omega)^2 d\mathbf{r} - \frac{1}{2}\beta \int \delta\omega \delta\psi d\mathbf{r} < 0, \quad (10)$$

for all perturbations  $\delta\omega$  that conserve energy and circulation at first order. In that case, it is formally nonlinearly dynamically stable with respect to the 2D Euler equations. This criterion is stronger than the well-known Arnol'd theorems that only provide sufficient conditions of stability. We note, however, that the refined criterion (7) provides itself just a sufficient condition of nonlinear dynamical stability. An even more refined criterion of dynamical stability is given by the Kelvin-Arnol'd principle. A review of the connections between these different stability criteria has been recently given by Chavanis [34].

### 3 The minimum enstrophy principle

Let us consider the minimization of the enstrophy  $\Gamma_2 = \int \omega^2 d\mathbf{r}$  at fixed circulation and energy

$$\min_{\omega} \{\Gamma_2[\omega] \mid E[\omega] = E, \Gamma[\omega] = \Gamma\}. \quad (11)$$

The critical points are given by the variational principle

$$\delta\Gamma_2 + 2\beta\delta E + 2\alpha\delta\Gamma = 0, \quad (12)$$

where  $2\beta$  and  $2\alpha$  are Lagrange multipliers (the factor 2 has been introduced for compatibility with the results of Sec. 4.3). This yields

$$\omega = -\Delta\psi = -\beta\psi - \alpha. \quad (13)$$

This is a steady state of the 2D Euler equation characterized by a linear  $\omega - \psi$  relationship. On the other hand it is a (local) minimum of enstrophy at fixed energy and circulation iff

$$\int (\delta\omega)^2 d\mathbf{r} + \beta \int \delta\omega \delta\psi d\mathbf{r} > 0, \quad (14)$$

for all perturbations  $\delta\omega$  that conserve energy and circulation at first order.

There are several interpretations of the minimization principle (11)<sup>4</sup>:

(i) The minimum enstrophy principle was introduced in a phenomenological manner from a selective decay principle [14, 16, 17]. Due to a small viscosity, or other source of dissipation, the enstrophy (fragile integral) is dissipated while the energy and the circulation (robust integrals) are relatively well conserved<sup>5</sup>. It is then argued that the system should reach a minimum enstrophy state at fixed circulation and energy. Note that there is no real justification for this last assumption as discussed in [27]. Furthermore, the minimum potential enstrophy principle is difficult to justify in terms of viscous effects for the QG equations (see the Appendix of [44]).

(ii) If we view  $\Gamma_2$  as a Casimir of the form (6), the minimization principle (11) is equivalent to the maximization principle (7) for the pseudo entropy  $S = -\frac{1}{2}\Gamma_2$ . In this context, it determines a particular steady state of the 2D Euler equation that is nonlinearly dynamically stable according to the refined stability criterion of Ellis *et al.* [29]. This provides another justification of the minimization problem (11) in relation to the inviscid 2D Euler equation.

(iii) For inviscid flows, the microscopic enstrophy  $\Gamma_2^{f.g.} = \int \overline{\omega^2} d\mathbf{r}$  is conserved by the 2D Euler equation

<sup>4</sup> The following interpretations can be generalized to any functional of the form  $S = - \int C(\omega) d\mathbf{r}$  where  $C$  is convex [34].

<sup>5</sup> For example, if  $\nu$  denotes the viscosity, we find from the Navier-Stokes equations that  $\dot{\Gamma}_2 = -2\nu \int (\nabla\omega)^2 d\mathbf{r}$  which tends to a finite value when  $\nu \rightarrow 0$  while  $(\nabla\omega)^2 \rightarrow +\infty$  as the flow develops small scales. Therefore, the enstrophy decays. By contrast,  $\dot{E} = -\nu\Gamma_2$  tends to zero when  $\nu \rightarrow 0$  so that the energy is relatively well conserved.

but the macroscopic enstrophy  $\Gamma_2^{c.g.} = \int \bar{\omega}^2 d\mathbf{r}$  calculated with the coarse-grained vorticity decreases as enstrophy is lost in the fluctuations. Indeed, by Schwartz inequality:  $\Gamma_2^{c.g.} = \int \bar{\omega}^2 d\mathbf{r} \leq \int \bar{\omega}^2 d\mathbf{r} = \Gamma_2^{f.g.}$ . By contrast, the energy  $E = \frac{1}{2} \int \bar{\omega} \psi d\mathbf{r}$  and the circulation  $\Gamma = \int \bar{\omega} d\mathbf{r}$  calculated with the coarse-grained vorticity are approximately conserved. This suggests an inviscid minimum enstrophy principle based on the minimization of macroscopic enstrophy at fixed energy and circulation [26]. In this case, selective decay is due to the operation of coarse-graining, not viscosity.

In the following, we shall discuss some connections between the minimum enstrophy principle and the maximum entropy principle.

## 4 Connection between maximum entropy states and minimum enstrophy states

### 4.1 Energy-enstrophy statistical theory

Starting from a generically unstable or unsteady initial condition, the 2D Euler equations are known to develop a complicated mixing process leading ultimately to a quasi stationary state (QSS), a vortex or a jet, on the coarse-grained scale. In order to describe this QSS and the fluctuations around it, we must introduce a probabilistic description. Let us introduce the density probability  $\rho(\mathbf{r}, \sigma)$  of finding the vorticity level  $\omega = \sigma$  at position  $\mathbf{r}$ . Then, the local moments of vorticity are  $\bar{\omega}^n = \int \rho \sigma^n d\mathbf{r}$ . In the statistical mechanics approach of Miller-Robert-Sommeria [24,25], assuming that the system is strictly described by the 2D Euler equation (no forcing and no dissipation), the statistical equilibrium state is expected to maximize the mixing entropy

$$S[\rho] = - \int \rho \ln \rho d\mathbf{r} d\sigma, \quad (15)$$

while conserving all the invariants (energy and Casimirs) of the 2D Euler equation. This forms the standard MRS theory.

In the case of flows that are forced and dissipated at small scales, one may argue that forcing and dissipation will compensate each other in average so that the system will again achieve a QSS that is a stationary solution of the 2D Euler equation. This QSS will be selected by forcing and dissipation. This fact is vindicated both in experiments [35,36] and numerical simulations [45]. In order to describe the fluctuations around this state, one needs to go one step further and obtain the vorticity distribution. An idea is to keep the framework of the statistical theory but argue that forcing and dissipation will alter the constraints. More precisely, forcing and dissipation will select some particular relevant constraints among all the invariants of the ideal 2D Euler equation. These constraints will determine the mean flow and the fluctuations around it. For example, we argue that there exists physical situations in which only the conservation of energy, circulation

and microscopic enstrophy are relevant (and of course the normalization condition). We do not claim that such situations are universal but simply that they happen in some cases of physical interest. This seems to be the case for example in some oceanic situations [6,7,8,9,10,11,12,13,14,15,16,17,18,19,20] (see also [46] for recent studies). We shall therefore consider the maximization problem

$$\max_{\rho} \{S[\rho] \mid E, \Gamma, \Gamma_2^{f.g.}, \int \rho d\eta = 1\}, \quad (16)$$

where

$$E = \frac{1}{2} \int \bar{\omega} \psi d\mathbf{r} = \frac{1}{2} \int \psi \rho \sigma d\mathbf{r} d\sigma, \quad (17)$$

$$\Gamma = \int \bar{\omega} d\mathbf{r} = \int \rho \sigma d\mathbf{r} d\sigma, \quad (18)$$

$$\Gamma_2^{f.g.} = \int \bar{\omega}^2 d\mathbf{r} = \int \rho \sigma^2 d\mathbf{r} d\sigma. \quad (19)$$

The last constraint (19) will be called the microscopic (or fine-grained) enstrophy because it takes into account the fluctuations of the vorticity  $\omega$ . It is different from the macroscopic (or coarse-grained) enstrophy

$$\Gamma_2^{c.g.} = \int \bar{\omega}^2 d\mathbf{r}. \quad (20)$$

which ignores these fluctuations. We have

$$\Gamma_2^{f.g.} = \int \omega_2 d\mathbf{r} + \Gamma_2^{c.g.}, \quad (21)$$

where  $\omega_2 \equiv \bar{\omega}^2 - \bar{\omega}^2$  is the local centered variance of the vorticity. The fluctuations of enstrophy are  $\Gamma_2^{fluct} = \int \omega_2 d\mathbf{r}$ . In our terminology, the enstrophy will be called a *fragile constraint* because it cannot be expressed in terms of the coarse-grained field since  $\bar{\omega}^2 \neq \bar{\omega}^2$ . While the microscopic enstrophy  $\Gamma_2^{f.g.}$  is conserved, the macroscopic enstrophy  $\Gamma_2^{c.g.}$  is not conserved and decays. By contrast, the energy (17) and the circulation (18) will be called *robust constraints* because they can be expressed in terms of the coarse-grained fields. We shall come back to this important distinction in Sec. 4.3.

The maximization problem (16) is what we shall call “the energy-enstrophy statistical theory”, or simply, “the statistical theory” in this paper. We note that a solution of (16) is always a MRS statistical equilibrium state, but the reciprocal is wrong in case of ensemble inequivalence because we have relaxed some constraints (the other Casimirs). Here, we keep the robust constraints  $E$  and  $\Gamma$  and only *one* fragile constraint  $\Gamma_2^{f.g.}$ , the quadratic one. We assume that these constraints are selected by the properties of forcing and dissipation. As we shall see, this assumption leads to Gaussian fluctuations and a mean flow characterized by a linear  $\bar{\omega} - \psi$  relationship. In principle, we can obtain more complex fluctuations and more

complex mean flows (characterized by nonlinear  $\bar{\omega} - \psi$  relationships) by keeping more and more fine-grained moments  $\Gamma_{n>1}^{f.g.}$  among the constraints. This can be a practical way to go beyond the Gaussian approximation. However, the Gaussian approximation, leading to a linear  $\bar{\omega} - \psi$  relationship, is already an interesting problem presenting rich bifurcations (because the energy constraint is nonlinear) [26], so that we shall stick to that situation.

The critical points of (16) are solution of the variational principle

$$\delta S - \beta \delta E - \alpha \delta \Gamma - \alpha_2 \delta \Gamma_2^{f.g.} - \int \zeta(\mathbf{r}) \delta \left( \int \rho d\eta \right) d\mathbf{r} = 0, \quad (22)$$

where  $\beta$ ,  $\alpha$ ,  $\alpha_2$  and  $\zeta(\mathbf{r})$  are Lagrange multipliers. This yields the Gibbs state

$$\rho(\mathbf{r}, \sigma) = \frac{1}{Z(\mathbf{r})} e^{-\alpha_2 \sigma^2} e^{-(\beta \psi + \alpha) \sigma}, \quad (23)$$

where the “partition function” is determined via the normalization condition

$$Z(\mathbf{r}) = \int e^{-\alpha_2 \sigma^2} e^{-(\beta \psi + \alpha) \sigma} d\sigma. \quad (24)$$

Therefore, in this approach, the distribution  $\rho(\mathbf{r}, \sigma)$  of the fluctuations of vorticity is Gaussian and the centered variance of the vorticity  $\omega_2(\mathbf{r})$  is uniform

$$\omega_2 \equiv \bar{\omega}^2 - \bar{\omega}^2 = \frac{1}{2\alpha_2} \equiv \Omega_2. \quad (25)$$

On the other hand, the mean flow is given by

$$\bar{\omega} = -\Omega_2(\beta \psi + \alpha). \quad (26)$$

This is a steady state of the 2D Euler equation characterized by a linear  $\bar{\omega} - \psi$  relationship. Then, the Gibbs state can be rewritten

$$\rho(\mathbf{r}, \sigma) = \frac{1}{\sqrt{2\pi\Omega_2}} e^{-\frac{(\sigma - \bar{\omega})^2}{2\Omega_2}}. \quad (27)$$

Since  $\omega_2 = \Omega_2$  is uniform at statistical equilibrium, we get

$$\Gamma_2^{f.g.} = \Omega_2 + \Gamma_2^{c.g.}. \quad (28)$$

Finally, a critical point of (16) is an entropy *maximum* at fixed  $E$ ,  $\Gamma$  and  $\Gamma_2^{f.g.}$  iff

$$\delta^2 J \equiv -\frac{1}{2} \int \frac{(\delta \rho)^2}{\rho} d\mathbf{r} d\sigma - \frac{1}{2} \beta \int \delta \bar{\omega} \delta \psi d\mathbf{r} < 0 \quad (29)$$

for all perturbations  $\delta \rho$  that conserve energy, circulation, microscopic enstrophy and normalization at first order (the proof is similar to the one given in [34] for related maximization problems).

*Remark:* From Eqs. (15) and (27), we easily find that  $S = \frac{1}{2} \ln \Omega_2$ . Then, using Eq. (28), we conclude that, at equilibrium, the entropy is given by

$$S = \frac{1}{2} \ln \left( \Gamma_2^{f.g.} - \Gamma_2^{c.g.} \right). \quad (30)$$

Therefore, if there exists several local entropy maxima (metastable states) for the same values of the constraints  $E$ ,  $\Gamma$  and  $\Gamma_2^{f.g.}$ , the maximum entropy state is the one with the smallest enstrophy  $\Gamma_2^{c.g.}$ . This is a first result showing connections between maximum entropy and minimum enstrophy principles. However, this *equilibrium* result does not prove that the maximization of the entropy functional  $S[\rho]$  at fixed  $E$ ,  $\Gamma$  and  $\Gamma_2^{f.g.}$  is equivalent to the minimization of the enstrophy functional  $\Gamma_2^{c.g.}[\bar{\omega}]$  at fixed  $E$  and  $\Gamma$  (e.g. an entropy maximum could be a saddle point of enstrophy). This equivalence will be shown in Sec. 4.3.

## 4.2 An equivalent but simpler variational principle

The maximization problem (16) is difficult to solve, especially regarding the stability condition (29), because we have to deal with a distribution  $\rho(\mathbf{r}, \sigma)$ . We shall introduce here an equivalent but simpler maximization problem by “projecting” the distribution on a smaller subspace. To solve the maximization problem (16), we can proceed in two steps<sup>6</sup>:

(i) *First step:* We first maximize  $S$  at fixed  $E$ ,  $\Gamma$ ,  $\Gamma_2^{f.g.}$ ,  $\int \rho d\sigma = 1$  and a given vorticity profile  $\bar{\omega}(\mathbf{r}) = \int \rho \sigma d\sigma$ . Since the specification of  $\bar{\omega}(\mathbf{r})$  determines  $E$  and  $\Gamma$ , this is equivalent to maximizing  $S$  at fixed  $\Gamma_2^{f.g.}$ ,  $\int \rho d\sigma = 1$  and  $\bar{\omega}(\mathbf{r}) = \int \rho \sigma d\sigma$ . Writing the variational problem as

$$\delta S - \alpha_2 \delta \Gamma_2^{f.g.} - \int \lambda(\mathbf{r}) \delta \left( \int \rho \sigma d\sigma \right) d\mathbf{r} - \int \zeta(\mathbf{r}) \delta \left( \int \rho d\sigma \right) d\mathbf{r} = 0, \quad (31)$$

we obtain

$$\rho_1(\mathbf{r}, \sigma) = \frac{1}{\sqrt{2\pi\Omega_2}} e^{-\frac{(\sigma - \bar{\omega})^2}{2\Omega_2}}, \quad (32)$$

with

$$\omega_2 \equiv \bar{\omega}^2 - \bar{\omega}^2 = \frac{1}{2\alpha_2} \equiv \Omega_2. \quad (33)$$

Note that the centered variance of the vorticity  $\omega_2(\mathbf{r}) = \Omega_2$  is *uniform*. Equation (33) also implies that  $\alpha_2$  must be positive. We check that  $\rho_1$  is a global entropy maximum with the previous constraints since  $\delta^2 S = -\int \frac{(\delta \rho)^2}{2\rho} d\mathbf{r} d\sigma < 0$  (the constraints are linear in  $\rho$  so their second variations vanish). Using the optimal distribution (32), we can express the entropy (15) in terms of  $\bar{\omega}$  writing  $S[\bar{\omega}] \equiv S[\rho_1]$ . After straightforward calculations we obtain

$$S = \frac{1}{2} \ln \Omega_2, \quad (34)$$

up to some unimportant constant terms. Note that  $\Omega_2$  is determined by the constraint on the microscopic enstrophy which leads to

$$\Omega_2 = \Gamma_2^{f.g.} - \int \bar{\omega}^2 d\mathbf{r}. \quad (35)$$

<sup>6</sup> This “two-steps” method was used by one of us (PHC) in different contexts [31, 47, 34].

The second term is the macroscopic enstrophy associated with the coarse-grained flow:  $\Gamma_2^{c.g.} = \int \bar{\omega}^2 d\mathbf{r}$ . The relation (35) can be used to express the entropy (34) in terms of  $\bar{\omega}$  alone.

(ii) *Second step:* we now have to solve the maximization problem

$$\max_{\bar{\omega}} \{S[\bar{\omega}] \mid E, \Gamma, \Gamma_2^{f.g.}\}, \quad (36)$$

with

$$S = \frac{1}{2} \ln \left( \Gamma_2^{f.g.} - \int \bar{\omega}^2 d\mathbf{r} \right), \quad (37)$$

$$E = \frac{1}{2} \int \bar{\omega} \psi d\mathbf{r}, \quad (38)$$

$$\Gamma = \int \bar{\omega} d\mathbf{r}. \quad (39)$$

The functional (37) might be called a generalized entropy. Interestingly, it resembles the Renyi entropy [38,39].

(iii) *Conclusion:* finally, the solution of (16) is given by (32) where  $\bar{\omega}$  is determined by (36). Therefore, (16) and (36) are equivalent but (36) is easier to solve because it is expressed in terms of  $\bar{\omega}(\mathbf{r})$  while (16) is expressed in terms of  $\rho(\mathbf{r}, \sigma)$ .

Up to second order, the variations of entropy (37) are given by

$$\Delta S = -\frac{1}{\Omega_2} \left( \int \bar{\omega} \delta \bar{\omega} d\mathbf{r} + \frac{1}{2} \int (\delta \bar{\omega})^2 d\mathbf{r} \right) - \frac{1}{(\Omega_2)^2} \left( \int \bar{\omega} \delta \bar{\omega} d\mathbf{r} \right)^2, \quad (40)$$

where  $\Omega_2$  is given by Eq. (35). Considering the first order variations of the entropy, the critical points of (36) are determined by the variational problem

$$\delta S - \beta \delta E - \alpha \delta \Gamma = 0. \quad (41)$$

This yields

$$\bar{\omega} = -\Omega_2(\beta\psi + \alpha). \quad (42)$$

We recover Eq. (26) for the mean flow. Combined with Eq. (32), we recover the Gibbs state (23). Considering now the second order variations of the entropy (40), we find that a critical point of (36) is a maximum of entropy at fixed energy, circulation and microscopic enstrophy iff

$$-\frac{1}{2\Omega_2} \int (\delta \bar{\omega})^2 d\mathbf{r} - \frac{\beta}{2} \int \delta \bar{\omega} \delta \psi d\mathbf{r} - \frac{1}{(\Omega_2)^2} \left( \int \bar{\omega} \delta \bar{\omega} d\mathbf{r} \right)^2 < 0, \quad (43)$$

for all perturbations  $\delta \bar{\omega}$  that conserve circulation and energy at first order (the conservation of microscopic enstrophy is automatically taken into account in our formulation). This stability condition is equivalent to Eq. (29)

but much simpler because it depends only on the perturbation  $\delta \bar{\omega}$  instead of the perturbation of the full distribution  $\delta \rho$ . In fact, the stability condition (43) can be simplified further. Indeed, using Eq. (42), we find that the term in parenthesis can be written

$$\int \bar{\omega} \delta \bar{\omega} d\mathbf{r} = -\Omega_2 \int (\beta\psi + \alpha) \delta \bar{\omega} d\mathbf{r}, \quad (44)$$

and it vanishes since the energy and the circulation are conserved at first order so that  $\delta E = \int \psi \delta \omega d\mathbf{r} = 0$  and  $\delta \Gamma = \int \delta \omega d\mathbf{r} = 0$ . Therefore, a critical point of (36) is a maximum of entropy at fixed energy, circulation and microscopic enstrophy iff

$$-\frac{1}{2\Omega_2} \int (\delta \bar{\omega})^2 d\mathbf{r} - \frac{\beta}{2} \int \delta \bar{\omega} \delta \psi d\mathbf{r} < 0, \quad (45)$$

for all perturbations  $\delta \bar{\omega}$  that conserve circulation and energy at first order. In fact, this stability condition can be obtained more rapidly if we remark that the maximization problem (36) is equivalent to the minimization of the macroscopic enstrophy at fixed energy and circulation (see Sec. 4.3).

#### 4.3 Equivalence with the minimum enstrophy principle

Since  $\ln(x)$  is a monotonically increasing function, it is clear that the maximization problem (36) is equivalent to

$$\max_{\bar{\omega}} \{S[\bar{\omega}] \mid E, \Gamma\}, \quad (46)$$

with

$$S = -\frac{1}{2} \Gamma_2^{c.g.}, \quad (47)$$

$$\Gamma_2^{c.g.} = \int \bar{\omega}^2 d\mathbf{r}, \quad (48)$$

$$E = \frac{1}{2} \int \bar{\omega} \psi d\mathbf{r}, \quad (49)$$

$$\Gamma = \int \bar{\omega} d\mathbf{r}. \quad (50)$$

The functional  $S$  of the coarse-grained vorticity  $\bar{\omega}$  is called a “generalized entropy”. It is proportional to the opposite of the coarse-grained enstrophy. We have the equivalences

$$(46) \Leftrightarrow (36) \Leftrightarrow (16). \quad (51)$$

Therefore, the maximization of MRS entropy at fixed energy, circulation and microscopic enstrophy is equivalent to the minimization of macroscopic enstrophy at fixed energy and circulation. The solution of (16) is given by Eq. (32) where  $\bar{\omega}$  is determined by (46) and  $\Omega_2$  by Eq. (35). Therefore, (16) and (46) are equivalent but (46) is easier to solve because it is expressed in terms of  $\bar{\omega}$  while (16) is expressed in terms of  $\rho$ . This provides a justification of the coarse-grained minimum enstrophy principle in terms of statistical mechanics when only the microscopic enstrophy is conserved among the Casimirs. Note that,



according to (7), the principle (46) also assures that the mean flow associated with the statistical equilibrium state (16) is nonlinearly dynamically stable with respect to the 2D Euler equation.

The critical points of (46) are given by the variational problem

$$\delta S - \beta \delta E - \alpha \delta \Gamma = 0. \quad (52)$$

This yields

$$\bar{\omega} = -\beta\psi - \alpha. \quad (53)$$

This returns Eq. (26) for the mean flow (up to a trivial redefinition of  $\beta$  and  $\alpha$ ). Together with Eq. (32), this returns the Gibbs state (23). On the other hand, this state is a maximum of  $S$  at fixed  $E$  and  $\Gamma$  iff

$$-\frac{1}{2} \int (\delta\bar{\omega})^2 d\mathbf{r} - \frac{\beta}{2} \int \delta\bar{\omega} \delta\psi d\mathbf{r} < 0, \quad (54)$$

for all perturbations  $\delta\bar{\omega}$  that conserve circulation and energy at first order. This is equivalent to the criterion (45) as it should.

We have thus shown the equivalence between the maximization of MRS entropy at fixed energy, circulation and fine-grained enstrophy with the minimization of coarse-grained enstrophy at fixed energy and circulation. This equivalence has been shown here for global maximization. In Appendix A, we prove the equivalence for local maximization by showing that the stability criteria (29) and (54) are equivalent.

*Remark:* In the framework of the MRS theory where all the Casimirs are conserved, the minimization of coarse-grained enstrophy at fixed energy and circulation provides a *sufficient* condition of MRS thermodynamical stability for initial conditions leading to a Gaussian vorticity distribution at equilibrium [32, 34, 48]. However, the reciprocal is wrong in case of “ensemble inequivalence” between microcanonical and grand microcanonical ensembles. In the framework of the EHT theory where the conservation of the Casimirs is replaced by the specification of a prior distribution, the minimization of coarse-grained enstrophy at fixed energy and circulation provides a *necessary and sufficient* condition of EHT thermodynamical stability for a Gaussian prior [31, 48].

#### 4.4 Equivalence with a grand microcanonical ensemble

In the basic maximization problem (16), the fine-grained enstrophy is treated as a constraint. Let us introduce a grand microcanonical ensemble by making a Legendre transform of the entropy with respect to this fragile constraint  $\Gamma_2^{f.g.}$  [34]. We thus introduce the functional  $S_g = S - \alpha_2 \Gamma_2^{f.g.}$  and the maximization problem

$$\max_{\rho} \{S_g[\rho] \mid E, \Gamma, \int \rho d\eta = 1\}. \quad (55)$$

A solution of (55) is always a solution of the more constrained dual problem (16) but the reciprocal is wrong in case of “ensemble inequivalence” [34]. In the present

case, however, we shall show that the microcanonical ensemble (16) and the grand microcanonical ensemble (55) are equivalent. This is because only a quadratic constraint (enstrophy) is involved.

To solve the maximization problem (55) we can proceed in two steps. We first maximize  $S_g$  at fixed  $E$ ,  $\Gamma$ ,  $\int \rho d\eta = 1$  and  $\bar{\omega}(\mathbf{r}) = \int \rho \sigma d\sigma$ . This is equivalent to maximizing  $S_g$  at fixed  $\int \rho d\eta = 1$  and  $\bar{\omega}(\mathbf{r}) = \int \rho \sigma d\sigma$ , and this leads to the optimal distribution (32) where  $\Omega_2 = 1/(2\alpha_2)$  is now fixed. This is clearly the global maximum of  $S_g$  with the previous constraints. Using this optimal distribution, we can now express the functional  $S_g$  in terms of  $\bar{\omega}$  by writing  $S[\bar{\omega}] = S_g[\rho_1]$ . After straightforward calculations, we obtain

$$S_g = -\frac{1}{2\Omega_2} \Gamma_2^{c.g.}, \quad (56)$$

up to some constant terms (recall that  $\Omega_2$  is a fixed parameter in the present situation). In the second step, we have to solve the maximization problem

$$\max_{\bar{\omega}} \{S[\bar{\omega}] \mid E, \Gamma\}. \quad (57)$$

Finally, the solution of (55) is given by (32) where  $\bar{\omega}$  is determined by (57). Therefore, the variational principle (55) is equivalent to (57). That this is true also for local maximization is shown in Appendix B of [48] (in a more general situation). On the other hand, since  $\Omega_2 > 0$ , the maximization problem (57) is equivalent to (46). Since we have proven previously that (46) is equivalent to the microcanonical variational principle (16), we conclude that (16) and (55) are equivalent.

## 5 Phase transitions in 2D Euler flows

### 5.1 Minimum enstrophy states

In this section we study the maximization problem

$$\max_{\bar{\omega}} \{S[\bar{\omega}] \mid E, \Gamma\}, \quad (58)$$

where  $S = -\frac{1}{2} \int \omega^2 d\mathbf{r}$  is the neg-enstrophy (the opposite of the enstrophy),  $E = \frac{1}{2} \int \omega \psi d\mathbf{r}$  the energy and  $\Gamma = \int \omega d\mathbf{r}$  the circulation. The maximization problem (58) can be interpreted as: (i) a criterion of nonlinear dynamical stability with respect to the 2D Euler equation (Sec. 2), (ii) a phenomenological minimum enstrophy principle (Sec. 3), (iii) a sufficient condition of MRS thermodynamical stability [32, 34], (iv) a necessary and sufficient condition of EHT thermodynamical stability for a Gaussian prior [34, 48], (v) a necessary and sufficient condition of thermodynamical stability in the energy-enstrophy statistical theory where only the microscopic enstrophy is conserved among the Casimirs (Sec. 4). For simplicity and convenience, we shall call  $S$  the entropy.

We write the variational principle for the first order variations as

$$\delta S - \beta \delta E - \alpha \delta \Gamma = 0, \quad (59)$$

where  $\beta$  and  $\alpha$  are Lagrange multipliers. This yields a linear  $\omega - \psi$  relationship

$$\omega = -\Delta\psi = -\beta\psi - \alpha. \quad (60)$$

As before, we assume that the area of the domain is unity and we set  $\langle X \rangle = \int X d\mathbf{r}$ . Taking the space average of Eq. (60), we obtain  $\Gamma = -\beta\langle\psi\rangle - \alpha$  so that the foregoing equation can be rewritten

$$-\Delta\psi + \beta\psi = \Gamma + \beta\langle\psi\rangle, \quad (61)$$

with  $\psi = 0$  on the domain boundary<sup>7</sup>. This is the fundamental differential equation of the problem. The energy and the entropy can then be expressed as

$$E = -\frac{1}{2}\beta(\langle\psi^2\rangle - \langle\psi\rangle^2) + \frac{1}{2}\Gamma\langle\psi\rangle, \quad (62)$$

$$S = -\frac{1}{2}\beta^2(\langle\psi^2\rangle - \langle\psi\rangle^2) - \frac{1}{2}\Gamma^2. \quad (63)$$

We shall study the maximization problem (58) by adapting the approach of Chavanis & Sommeria [26] to this specific situation (these authors studied a related but not exactly equivalent problem). We will see that the structure of the problem depends on a unique control parameter [26]:

$$\Lambda = \frac{\Gamma}{\sqrt{2E}}. \quad (64)$$

We note that the maximization problem (58) has been studied recently by Venaille & Bouchet [40] by using a different theoretical treatment. They performed a detailed analysis of the phase transitions associated with (58) in the context of statistical mechanics, emphasizing in particular the notion of ensemble inequivalence. However, their approach is very abstract. Our study is more direct and can offer a complementary discussion of the problem. The maximization problem (58) has also been studied recently by Keetels *et al.* [41] with different boundary conditions adapted to viscous flows.

## 5.2 The bifurcation diagram

In this section, we apply the methodology developed by Chavanis & Sommeria [26]. This methodology is relatively general: it is valid for an arbitrary domain and for an arbitrary linear operator. However, for illustration, we shall consider the Laplacian operator and a rectangular domain.

<sup>7</sup> As mentioned in the introduction, our approach assumes that forcing and dissipation equilibrate each other so that the system becomes, in average, statistically equivalent to the 2D Euler equation. Therefore, we use boundary conditions consistent with the 2D Euler equation. However, our approach is expected to be valid only in the bulk of the flow, relatively far from the boundary layers where our assumptions do not hold anymore. Therefore, the boundary that we consider may not correspond to the true, physical, boundary of the fluid, but may be an “effective domain” where our inviscid assumption applies. For further discussion on the influence of boundary conditions on the structure of the flow, see Keetels *et al.* [41] and references therein.

### 5.2.1 The eigenmodes

We first assume that

$$\Gamma + \beta\langle\psi\rangle = 0, \quad (65)$$

corresponding to  $\alpha = 0$ . In that case, the differential equation (61) becomes

$$-\Delta\psi + \beta\psi = 0, \quad (66)$$

with  $\psi = 0$  on the domain boundary. Using the results of Appendix B, Eq. (66) has solutions only for  $\beta = \beta_{mn}$  (eigenvalues) and the corresponding solutions (eigenfunctions) are

$$\psi = \left(\frac{2E}{-\beta_{mn}}\right)^{1/2} \psi_{mn}, \quad (67)$$

where we have used the energy constraint (62) to determine the normalization constant. Substituting this result in Eq. (65), we find that these solutions exist only for  $\Lambda = \Lambda_{mn}$  with

$$\Lambda_{mn}^2 = -\beta_{mn}\langle\psi_{mn}\rangle^2. \quad (68)$$

For the eigenmodes  $\langle\psi_{mn}\rangle = 0$  ( $m$  or  $n$  even), we find  $\Lambda = 0$  and for the eigenmodes  $\langle\psi_{mn}\rangle \neq 0$  ( $m$  and  $n$  odd), we find  $\Lambda^2 = \Lambda_{mn}^{\prime\prime 2} = -\beta_{mn}\langle\psi_{mn}\rangle^2 \neq 0$ .

### 5.2.2 The solutions of the continuum

We now assume that  $\Gamma + \beta\langle\psi\rangle \neq 0$  and we define

$$\phi = \frac{\psi}{\Gamma + \beta\langle\psi\rangle}. \quad (69)$$

In that case, the differential equation (61) becomes

$$-\Delta\phi + \beta\phi = 1, \quad (70)$$

with  $\phi = 0$  on the domain boundary. We also assume that  $\beta \neq \beta_{mn}$ . In that case, Eq. (70) has a unique solution that can be obtained by expanding  $\phi$  on the eigenmodes. We get

$$\phi = \sum_{mn} \frac{\langle\psi_{mn}\rangle}{\beta - \beta_{mn}} \psi_{mn}, \quad (71)$$

where only the modes with  $\langle\psi_{mn}\rangle \neq 0$  are “excited”.

For  $\Gamma \neq 0$ , taking the average of Eq. (69) and solving for  $\langle\psi\rangle$ , we obtain  $\langle\psi\rangle = \Gamma\langle\phi\rangle/(1 - \beta\langle\phi\rangle)$ . Therefore, the solution of Eq. (61) is

$$\psi = \frac{\Gamma\phi}{1 - \beta\langle\phi\rangle}. \quad (72)$$

Substituting this solution in the energy constraint (62), we obtain the “equation of state”:

$$(1 - \beta\langle\phi\rangle)^2 = \Lambda^2(\langle\phi\rangle - \beta\langle\phi^2\rangle). \quad (73)$$

This equation determines  $\beta$  as a function of  $\Lambda$ . In particular, it determines the caloric curve  $\beta(E)$  for a given value of  $\Gamma \neq 0$ . Note that the equation of state involves the important function [26]:

$$F(\beta) \equiv \beta \langle \phi \rangle - 1. \quad (74)$$

For  $\Gamma = 0$ , the solution of Eq. (61) is

$$\psi = \beta \langle \psi \rangle \phi. \quad (75)$$

Taking the space average of this relation, we find that this solution exists only for a discrete set of temperatures  $\beta = \beta_*^{(k)}$  satisfying  $F(\beta_*^{(k)}) = 0$ . We shall note  $\beta_* \equiv \beta_*^{(1)}$  the largest of these solutions. Substituting Eq. (75) in the energy constraint (62), we find that the amplitude  $\langle \psi \rangle$  is determined by

$$E = -\frac{1}{2} \beta^3 \langle \psi \rangle^2 (\langle \phi^2 \rangle - \langle \phi \rangle^2). \quad (76)$$

Of course, the case  $\Lambda = 0$  is also a limit case of the equation of state (73).

### 5.2.3 The mixed solutions

For  $\beta \rightarrow \beta_{mn}$  with  $m$  and  $n$  odd ( $\langle \psi_{mn} \rangle \neq 0$ ), we find from Eq. (71) that  $\phi \sim \langle \psi_{mn} \rangle \psi_{mn} / (\beta - \beta_{mn}) \rightarrow +\infty$  leading to  $\Lambda \rightarrow \Lambda'_{mn}$  and  $\psi \rightarrow (2E/\beta_{mn})^{1/2} \psi_{mn}$ . Therefore, we recover the eigenfunction  $\psi_{mn}$  as a limit case. The eigenfunctions with non vanishing average value are therefore contained on the continuum branch.

For  $\beta = \beta_{mn}$  with  $m$  or  $n$  even ( $\langle \psi_{mn} \rangle = 0$ ), the solution of Eq. (70) is not unique. It corresponds to the mixed solutions

$$\phi = \sum_{m'n'} \frac{\langle \psi_{m'n'} \rangle}{\beta_{mn} - \beta_{m'n'}} \psi_{m'n'} + \chi_{mn} \psi_{mn}, \quad (77)$$

where  $\chi_{mn}$  is determined by the energy constraint (more precisely, it can be related to  $\Lambda$  by substituting Eq. (77) in Eq. (73) where now  $\beta = \beta_{mn}$ ). These solutions form a plateau at fixed temperature  $\beta = \beta_{mn}$ . For  $\chi_{mn} \rightarrow +\infty$ , we recover the pure eigenmode  $\psi_{mn}$  that exists at  $\Lambda = 0$  and for  $\chi_{mn} = 0$ , we connect the branch of continuum solutions at  $\Lambda = \Lambda'_{mn}$ .

The general bifurcation diagram showing the eigenmodes, the solutions of the continuum and the mixed solutions is represented in Fig. 2 of [26] (see also Figs. 1 and 2 below).

### 5.3 The geometry induced monopole/dipole transition

For a given value of the control parameter  $\Lambda$ , we can have an infinite number of solutions to Eq. (61) [26]. We can now use the entropy (63) to select the most probable state (maximum entropy state) among all these solutions.

For the eigenmodes, the entropy takes the simple form  $S/E = \beta_{mn}$ . In particular, for the eigenmodes  $\psi_{mn}$  with

$m$  or  $n$  even ( $\langle \psi_{mn} \rangle = 0$ ) that exist only for  $\Lambda = 0$ , we have

$$\frac{S}{E}(\Lambda = 0) = \beta_{mn}. \quad (78)$$

For a rectangular domain elongated in the  $x$  direction, the eigenmode with the highest entropy at  $\Gamma = 0$  is the dipole  $(m, n) = (2, 1)$  with temperature  $\beta_{21}(\tau)$ . Therefore, the maximum entropy state (or the minimum enstrophy state) corresponds to the mode with the largest scale. The modes with smaller scales ( $m, n$  large) have lower entropy (higher enstrophy). Therefore, the maximum entropy and minimum enstrophy principles select the large-scale structures among the infinite class of steady states of the 2D Euler equation. This is a manifestation of the inverse cascade process.

For the solutions of the continuum, the entropy can be written

$$S/E = \beta \left( 1 + \Lambda^2 \frac{\langle \phi \rangle}{\beta \langle \phi \rangle - 1} \right) - \Lambda^2. \quad (79)$$

For  $\Lambda = 0$ , this expression reduces to

$$\frac{S}{E}(\Lambda = 0) = \beta_*^{(k)}. \quad (80)$$

The solution with highest entropy is the monopole with temperature  $\beta_*(\tau)$ .

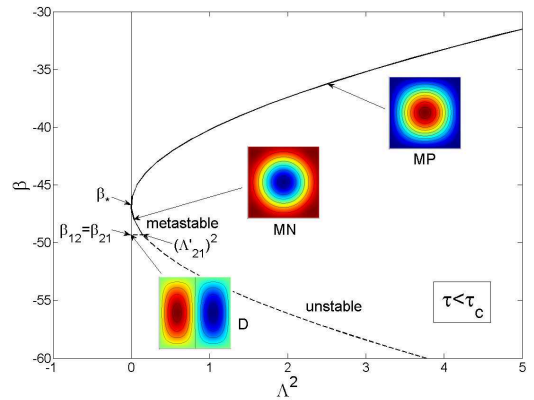


**Fig. 1.** Series of equilibria in a square domain ( $\tau = 1 < \tau_c$ ). In that case  $\max\{\beta_*, \beta_{21}\} = \beta_*$ . The maximum entropy state is the direct monopole (for  $\Gamma > 0$  the vorticity is positive at the center and negative at the periphery (MP); for  $\Gamma < 0$  this is the opposite (MN)) for any value of  $\Lambda^2$ . For  $\Lambda^2 < (\Lambda'_{21})^2$ , the reversed monopole is metastable (local entropy maximum) as discussed in Sec. 5.4. Note that the metastable states have negative specific heats  $C = \frac{\partial E}{\partial T} = \beta^2 E^2 \frac{\partial(1/E)}{\partial \beta} < 0$ . For  $\Gamma = 0$ , the direct and reversed monopoles have the same entropy. For fixed  $\Gamma$ , the caloric curve  $\beta(E)$  does not present any phase transition (see Sec. 5.6). The vorticity profiles are plotted for  $\Gamma \geq 0$ . The red colour corresponds to positive values of the vorticity and the blue colour to negative values.

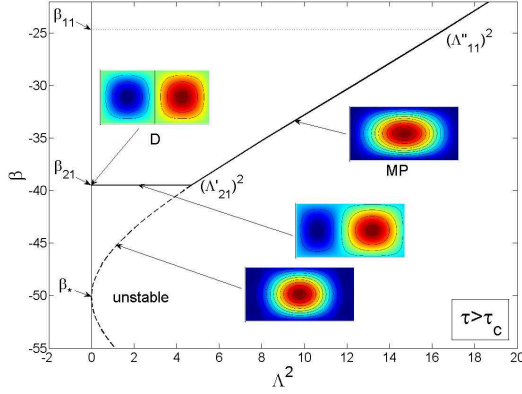


**Fig. 2.** Series of equilibria in a rectangular domain with aspect ratio  $\tau = 2 > \tau_c$ . In that case  $\max\{\beta_*, \beta_{21}\} = \beta_{21}$ . The maximum entropy state is the dipole for  $\Lambda^2 < (\Lambda'_{21})^2$  and the direct monopole for  $\Lambda^2 > (\Lambda'_{21})^2$  (the reversed monopoles are unstable). For  $\Gamma \neq 0$ , the caloric curve  $\beta(E)$  presents a second order phase transition marked by the discontinuity of  $\frac{\partial \beta}{\partial E}(E)$  at  $E = E'_{21}$  as discussed in Sec. 5.6.

For  $\Lambda = 0$ , we have a competition between the monopole  $\beta_*(\tau)$  (continuum branch) and the dipole  $\beta_{21}(\tau)$  (eigenmode)<sup>8</sup>. We must therefore compare their entropy (or equivalently their inverse temperature) to select the maximum entropy state. As shown in Chavanis & Sommeria [26], this selection depends on the geometry of the domain. In a rectangular domain, it is found that the monopole has the highest entropy ( $\beta_* > \beta_{21}$ ) for  $\tau < \tau_c = 1.12$  while the dipole dominates ( $\beta_{21} > \beta_*$ ) for  $\tau > \tau_c = 1.12$ . More generally, it can be shown that the entropy is a monotonically increasing function of the inverse temperature (for a fixed value of  $\Lambda$ ). Therefore, at any  $\Lambda$ , the maximum entropy state is the one with the highest inverse temperature [26]. The series of equilibria  $\beta(\Lambda)$  is represented in Figs. 1 and 2 for a square domain and for a rectangular domain of aspect ratio 2, respectively. For  $\tau < \tau_c$ , the maximum entropy state is the direct monopole for any value of  $\Lambda$ . For  $\tau > \tau_c$ , the maximum entropy state is the dipole for  $\Lambda^2 < (\Lambda'_{21})^2$  and the direct monopole for  $\Lambda^2 > (\Lambda'_{21})^2$ .

#### 5.4 Stability analysis and ensemble inequivalence

For given values of  $E$  and  $\Gamma$ , there can exist different critical points of entropy  $S$  (canceling its first order variations). They are solutions of the differential equation (61). For sufficiently small  $\Lambda$ , there exists an infinity of solutions [26]. In the last section, we have compared the value of the entropy of these different solutions in order to select the maximum entropy state. However, a more precise study

<sup>8</sup> As noted by Taylor *et al.* [42], the solution with  $\langle \psi \rangle = 0$  (dipole) has zero angular momentum while the solution with  $\langle \psi \rangle \neq 0$  (monopole) has nonzero angular momentum, even though the circulation is zero. This explains the “spin-up” phenomenon discovered in [43].

should determine which solutions correspond to global entropy maxima, local entropy maxima and saddle points. Saddle points of entropy are unstable and should be rejected in principle (see, however Sec. 6.2). By contrast, local entropy maxima (metastable states) can be long-lived for systems with long-range interactions. In practice, they are as much relevant as global entropy maxima (stable states). In the following, using an approach very close to the one followed by Chavanis & Sommeria [26] (but not exactly equivalent since the variational problems differ), we determine sufficient conditions of *instability*. This will eliminate a large class of solutions that are unstable saddle points of entropy and give the form of the perturbations that destabilize them. The remaining solutions are either stable or metastable.

A critical point of entropy at fixed energy and circulation is a (local) maximum iff

$$\delta^2 J = - \int \frac{(\delta\omega)^2}{2} d\mathbf{r} - \frac{1}{2} \beta \int \delta\omega \delta\psi d\mathbf{r} < 0, \quad (81)$$

for all perturbations that conserve energy and circulation at first order:  $\delta E = \delta \Gamma = 0$ .

(i) We first show that all the solutions with  $\beta < \beta_{21}$  are unstable (saddle points). To that purpose, we consider a perturbation of the form  $\delta\omega = \psi_{21}(\mathbf{r})$ . The corresponding stream function is  $\delta\psi = -\frac{1}{\beta_{21}}\psi_{21}(\mathbf{r})$ . For this perturbation, it is clear that  $\delta\Gamma = \int \delta\omega d\mathbf{r} = 0$  since  $\langle \psi_{21} \rangle = 0$ . Furthermore,  $\delta E = \int \psi \delta\omega d\mathbf{r} = 0$  since  $\psi_{21}$  is orthogonal to the other eigenmodes and to the solutions of the continuum (as they involve a summation (71) on the eigenmodes with non zero average that are orthogonal to  $\psi_{21}$ ). Finally, a simple calculation shows that

$$\delta^2 J = \frac{1}{2} \left( \frac{\beta}{\beta_{21}} - 1 \right) > 0. \quad (82)$$

We have thus found a particular perturbation that increases the entropy at fixed energy and circulation. Therefore, the states with  $\beta < \beta_{21}$  are unstable (saddle points).

(ii) We now show that if  $\beta_{21} < \beta_*$  the mode  $\psi_{21}$  existing at  $\Lambda = 0$  is unstable (saddle point). To that purpose, we consider a perturbation of the form  $\delta\omega = 1 - \beta_* \phi_*$  (where  $\phi_*$  is the solution of Eq. (70) corresponding to  $\beta = \beta_*$ ). The corresponding stream function is  $\delta\psi = \phi_*$ . For this perturbation, it is clear that  $\delta\Gamma = \int \delta\omega d\mathbf{r} = 0$  since  $1 - \beta_* \langle \phi_* \rangle = 0$ . Furthermore,  $\delta E = \int \psi_{21} \delta\omega d\mathbf{r} = 0$  since  $\langle \psi_{21} \rangle = 0$  and  $\psi_{21}$  is perpendicular to  $\phi_*$  as explained previously. Finally, after some simple algebra using  $1 - \beta_* \langle \phi_* \rangle = 0$ , we get

$$\delta^2 J = \frac{1}{2} (\beta_* - \beta_{21}) (\langle \phi_* \rangle - \beta_* \langle \phi_*^2 \rangle) > 0, \quad (83)$$

(the last term in parenthesis is positive as shown in Appendix B). We have thus found a particular perturbation that increases the entropy at fixed energy and circulation. Therefore, if  $\beta_{21} < \beta_*$  the mode  $\psi_{21}$  existing at  $\Lambda = 0$  is unstable. By continuity, the mixed solutions forming a plateau at  $\beta = \beta_{21}$  are also unstable if  $\beta_{21} < \beta_*$  since the two ends of the plateau are unstable.



The maximization problem (58) corresponds to a condition of microcanonical stability which is relevant to our problem since the circulation and the energy are conserved by the 2D Euler equation. However, it can be convenient to establish criteria of canonical and grand canonical stability. Indeed, the solution of a maximization problem is always solution of a more constrained dual maximization problem, but the reciprocal is wrong in case of ensemble inequivalence that is generic for systems with long-range interactions [33]. Therefore, conditions of canonical and grand canonical stability provide only *sufficient* conditions of microcanonical stability: grand canonical stability implies canonical stability which itself implies microcanonical stability (see, e.g., [34]). This problem of ensemble inequivalence has been studied in detail by Venaille & Bouchet [40] and we briefly discuss it again bringing some complements regarding the metastable states (that are not considered in [40]).

Considering the grand canonical ensemble, we have to maximize the grand potential  $G = S - \beta E - \alpha \Gamma$  (no constraint problem). The condition of grand canonical stability corresponds to inequality (81) for all variations  $\delta\omega$ . By decomposing the perturbation of the eigenmodes of the Laplacian, it is easy to show that the system is a maximum of grand potential iff  $\beta > \beta_{11}$  (where  $\beta_{11}$  is the largest eigenvalue of the Laplacian). This is closely related to the Arnol'd theorem (indeed, the grand potential is equivalent to the Arnol'd energy-Casimir functional [34]; furthermore, for a linear  $\omega - \psi$  relationship, the Arnol'd theorem, which usually provides only a sufficient condition of grand canonical stability, now provides a necessary and sufficient condition of grand canonical stability). Since grand canonical stability implies microcanonical stability (but not the converse) we conclude that, if  $\beta > \beta_{11}$ , the system is a maximum of entropy at fixed circulation and energy.

Considering the canonical ensemble, we have to maximize the free energy  $J = S - \beta E$  at fixed circulation (one constraint problem). The condition of canonical stability corresponds to inequality (81) for all variations  $\delta\omega$  that conserve circulation. By carefully taking into account the constraint on the circulation, Venaille & Bouchet [40] show that the system is a maximum of free energy iff  $\beta > \max\{\beta_{21}, \beta_*\}$ . In particular, the states with  $\max\{\beta_{21}, \beta_*\} < \beta < \beta_{11}$  are stable in the canonical ensemble but unstable in the grand canonical ensemble. Thus, canonical and grand canonical ensembles are inequivalent [40]. On the other hand, since canonical stability implies microcanonical stability (but not the converse) we conclude that, if  $\beta > \max\{\beta_{21}, \beta_*\}$ , the system is a maximum of entropy at fixed circulation and energy. In particular, the states with  $E > \Gamma^2/(2\Lambda_{11}^2) \equiv E_{11}(\Gamma)$  are stable in the canonical ensemble but unstable in the grand canonical ensemble [40]. Note that the states with  $\beta < \beta_*$  are unstable in the canonical ensemble (they are saddle points of free energy at fixed circulation). This result can be obtained directly by considering a perturbation of the form  $\delta\omega = 1 - \beta_*\phi_*$  like in (ii). For this perturbation,  $\delta\Gamma = 0$ . On the other hand, in the canonical ensemble, we do not

need to impose  $\delta E = 0$  so that this perturbation can be applied to *any* state leading to

$$\delta^2 J = \frac{1}{2}(\beta_* - \beta)(\langle\phi_*\rangle - \beta_*(\phi_*^2)) > 0, \quad (84)$$

which proves the result. By contrast, this argument does not work in the microcanonical ensemble since the chosen perturbation does not satisfy  $\delta E = 0$  for all states. Therefore, when  $\beta_* > \beta_{21}$ , the states with  $\beta_{21} < \beta < \beta_*$  are unstable in the canonical ensemble (they are saddle points of free energy at fixed circulation) while they are metastable in the microcanonical ensemble (they are local maxima of entropy at fixed circulation and energy). This is an interesting notion of ensemble inequivalence which affects metastable states (Venaille & Bouchet [40] show that the microcanonical and canonical ensembles are equivalent for the fully stable states but the case of metastable states is not considered in their study). In particular, we note that the metastable states with  $\beta_{21} < \beta < \beta_*$  have *negative specific heats* (see Fig. 1). This is allowed in the microcanonical ensemble but not in the canonical ensemble. Interestingly, this is the first observation of negative specific heats in that context.

Combining all these results, we conclude that in the microcanonical ensemble:

- (a) If  $\beta_{21} < \beta_*$ : the states are stable for  $\beta \geq \beta_*$ , unstable for  $\beta \leq \beta_{21}$  and metastable for  $\beta_{21} < \beta < \beta_*$ , as shown in Fig. 1. Therefore, the direct monopole is stable for any  $\Lambda^2$  and the reversed monopole is metastable for  $\Lambda^2 < (\Lambda'_{21})^2$ .
- (b) If  $\beta_{21} > \beta_*$ : the states are stable for  $\beta \geq \beta_{21}$  and unstable for  $\beta < \beta_{21}$ , as shown in Fig. 2. Therefore, the dipole is stable for  $\Lambda^2 < (\Lambda'_{21})^2$  and the direct monopole is stable for  $\Lambda^2 > (\Lambda'_{21})^2$ . There is no metastable state in that case.

## 5.5 The chemical potential

In Sec. 5.3, we have represented the inverse temperature  $\beta$  as a function of  $\Lambda$ . We shall now study how the chemical potential  $\alpha$  depends on  $\Lambda$ . The chemical potential is given by  $\alpha = -\beta\langle\psi\rangle - \Gamma$ . For the eigenmodes,

$$\alpha = 0. \quad (85)$$

For the solutions of the continuum, assuming  $\Gamma \neq 0$ , and using Eq. (72), we get  $\alpha = \Gamma/(\beta\langle\phi\rangle - 1) = \Gamma/F(\beta)$ . Therefore,

$$\frac{\alpha}{\sqrt{2E}} = \frac{\Lambda}{F(\beta)}. \quad (86)$$

For  $\Gamma = 0$ , using Eq. (75), we obtain

$$\frac{\alpha}{\sqrt{2E}} = \pm \frac{1}{\sqrt{-\beta_*(\langle\phi_*^2\rangle - \langle\phi_*\rangle^2)}}, \quad (87)$$

which is a limit case of Eq. (86). The normalized chemical potential  $\alpha/\sqrt{2E}$  is plotted as a function of  $\Lambda$  in Figs. 3

and 4, for a square domain and for a rectangular domain of aspect ratio 2, respectively. To plot this curve, we have used Eqs. (73) and (86). For a given value of  $\beta$ , we can determine  $\Lambda$  by Eq. (73) and  $\alpha/\sqrt{2E}$  by Eq. (86). Therefore, we can obtain  $\alpha/\sqrt{2E}$  as a function of  $\Lambda$  parameterized by  $\beta$  for the solutions of the continuum. For the mixed solutions,  $\beta = \beta_{mn}$  is fixed and  $\alpha/\sqrt{2E}$  is a linear function of  $\Lambda$  given by Eq. (86).

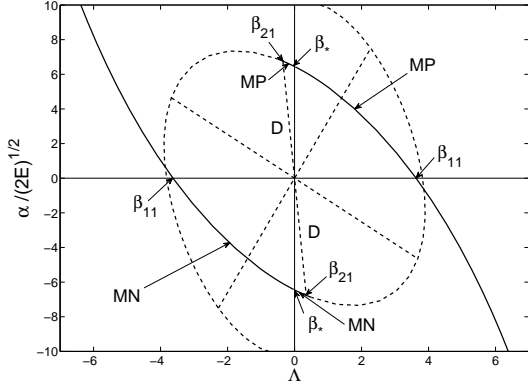


**Fig. 3.** Relationship between  $\alpha/\sqrt{2E}$  and  $\Lambda$  in a square domain (case  $\beta_{21} < \beta_*$ ). The solid lines correspond to the stable ( $\beta \geq \beta_*$ ) and metastable ( $\beta_{21} < \beta < \beta_*$ ) states. Unstable states ( $\beta \leq \beta_{21}$ ) are represented by the dashed lines. The straight lines represent the mixed solutions with constant temperature:  $\beta = \beta_{12} = \beta_{21}$ ,  $\beta = \beta_{22}$ ,  $\beta = \beta_{23}$ .

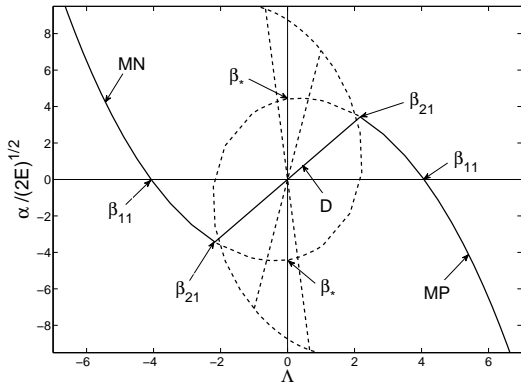


**Fig. 4.** Relationship between  $\alpha/\sqrt{2E}$  and  $\Lambda$  in a rectangular domain of aspect ratio 2 (case  $\beta_{21} > \beta_*$ ). The solid lines correspond to the stable states ( $\beta \geq \beta_{21}$ ). Unstable states ( $\beta < \beta_{21}$ ) are represented by the dashed lines. The straight lines represent the mixed solutions with constant temperature:  $\beta = \beta_{21}$ ,  $\beta = \beta_{12}$ ,  $\beta = \beta_{22}$ .

In Figs. 3 and 4, we have represented the series of equilibria containing all the critical points of entropy. If we continue the series of equilibria to more and more unstable states, the curve rolls up several times around the

origin (not shown). As indicated above, the series of equilibria is parameterized by  $\beta$ . The branches corresponding to  $\beta > \beta_{11}$  are stable in the grand canonical, canonical and microcanonical ensembles and the branches corresponding to  $\beta > \max\{\beta_{21}, \beta_*\}$  are stable in the canonical and microcanonical ensembles. The part of the branches corresponding to  $\max\{\beta_{21}, \beta_*\} < \beta < \beta_{11}$  are stable in the canonical and microcanonical ensembles but not in the grand canonical ensemble. For  $\tau < \tau_c$  ( $\beta_{21} < \beta_*$ ), the part of the branches corresponding to  $\beta_{21} < \beta < \beta_*$  are metastable in the microcanonical ensemble and unstable in the other ensembles.

*Remark:* in the grand canonical ensemble, the control parameter is the chemical potential  $\alpha$  and the conjugated variable is the circulation  $\Gamma$ . We must therefore consider  $\Gamma(\alpha)$  by rotating the curves of Figs. 3 and 4 by  $90^\circ$ . Only the part of the curve with  $\beta > \beta_{11}$  (NW and SE quadrants) are stable in the grand canonical ensemble. There is a first order grand canonical phase transition at  $\alpha = 0$  marked by the discontinuity of the circulation  $\Gamma(\alpha)$  between  $\Gamma = \pm \Lambda''_{11} \sqrt{2E}$ . Note that there is no metastable states in the grand canonical ensemble because the states with  $\beta < \beta_{11}$  are all unstable.

## 5.6 Description of phase transitions

We briefly discuss the nature of phase transitions associated with the maximization problem (58) and confirm the results that Venaille & Bouchet [40] obtained by a different method. We also give a special attention to the metastable states that are not considered in [40].

We shall describe successively the caloric curve  $\beta(E)$  for a fixed  $\Gamma$  and the chemical potential curve  $\alpha(\Gamma)$  for a fixed  $E$ . As first observed by Chavanis & Sommeria [26], the nature of the phase transitions depends on the value of  $\max\{\beta_*, \beta_{21}\}$ . In a rectangular domain, this quantity is determined by the value of the aspect ratio  $\tau$ . We must therefore consider two cases successively:  $\tau < \tau_c$  and  $\tau > \tau_c$ .

### 5.6.1 Caloric curve

The caloric curve corresponds to the stable part of the series of equilibria  $\beta(E)$  containing global (stable) and local (metastable) maximum entropy states at fixed  $E$  and  $\Gamma$ .

- Let us first consider  $\tau < \tau_c$  corresponding to  $\max\{\beta_*, \beta_{21}\} = \beta_*$  as in Fig. 1. For  $\Gamma = 0$ , the maximum entropy state is the monopole and the caloric curve is simply a straight line  $\beta(E, \Gamma = 0) = \beta_*$ . For each value of the energy, we have two solutions with the same inverse temperature  $\beta_*$  but different values of the chemical potential  $\alpha(\Gamma = 0, E) = \pm \alpha_0$  (see Fig. 3). One solution is a monopole with positive vorticity at the center (MP) and the other solution is a monopole with negative vorticity at the center (MN). For  $\Gamma = 0$ , these solutions have the same entropy. Thus, the branch  $\beta(E, \Gamma = 0) = \beta_*$  is degenerate. For  $\Gamma \neq 0$ , the caloric curve  $\beta(E, \Gamma \neq 0)$  can be deduced

easily from Fig. 1<sup>9</sup>. The global maximum entropy state is the direct monopole (for  $\Gamma > 0$  the vorticity is positive at the center (MP); for  $\Gamma < 0$  the vorticity is negative at the center (MN)) for any  $E$ . For  $E > E'_{21}(\Gamma) \equiv \frac{\Gamma^2}{2(\Lambda'_{21})^2}$ , the reversed monopole is metastable (local entropy maximum). Note that the metastable states have negative specific heats  $C \equiv dE/d(1/\beta) < 0$ . The caloric curve  $\beta(E)$  does not present any phase transition.

- Let us now consider  $\tau > \tau_c$  corresponding to  $\max\{\beta_*, \beta_{21}\} = \beta_{21}$  as in Fig. 2. For  $\Gamma = 0$ , the maximum entropy state is the dipole and the caloric curve is simply a straight line  $\beta(E, \Gamma = 0) = \beta_{21}$ . For each value of the energy, we have two solutions with the same inverse temperature and the same chemical potential  $\alpha(\Gamma = 0, E) = 0$  (see Fig. 4). One solution is a dipole  $(+, -)$  with positive vorticity on the left and the other solution is a dipole  $(-, +)$  with negative vorticity on the left (in Fig. 2, we have only represented the dipole  $(-, +)$ ). For  $\Gamma = 0$ , these solutions have the same entropy. Thus, the branch  $\beta(E, \Gamma = 0) = \beta_{21}$  is degenerate. For  $\Gamma \neq 0$ , the caloric curve  $\beta(E, \Gamma \neq 0)$  can be deduced easily from Fig. 2. The maximum entropy state is the asymmetric (mixed) dipole  $(+, -)$  or  $(-, +)$  for  $E > E'_{21}(\Gamma) \equiv \frac{\Gamma^2}{2(\Lambda'_{21})^2}$  and the direct monopole for  $E < E'_{21}(\Gamma) \equiv \frac{\Gamma^2}{2(\Lambda'_{21})^2}$  (the reversed monopoles are unstable). The caloric curve  $\beta(E)$  presents a second order phase transition marked by the discontinuity of  $\frac{\partial\beta}{\partial E}(E)$  at  $E = E'_{21}(\Gamma)$ .

### 5.6.2 Chemical potential curve

The chemical potential curve corresponds to the stable part of the series of equilibria  $\alpha(\Gamma)$  containing global (stable) and local (metastable) maximum entropy states at fixed  $E$  and  $\Gamma$ .

- Let us first consider  $\tau < \tau_c$  corresponding to  $\max\{\beta_*, \beta_{21}\} = \beta_*$  as in Fig. 3. The global maximum entropy state is the monopole for any value of  $\Gamma$ . Considering only fully stable states (global entropy maxima), there is a first order phase transition at  $\Gamma = 0$  marked by the discontinuity of  $\alpha(\Gamma)$  while the entropy is continuous. When we pass from positive  $\Gamma$  to negative  $\Gamma$ , we pass discontinuously (in terms of  $\alpha$  but not in terms of  $\beta$  or  $S$ ) from the monopole (MP) to the monopole (NP). In fact, due to the presence of long-lived metastable states (see Sec. 6.3), we remain in practice on the monopole (MP) until the metastable branch disappears. Then we jump on the monopole (MN) with discontinuity of  $\alpha$  (and  $\beta$  and  $S$ ). This corresponds to a zeroth order phase transition.

- Let us now consider  $\tau > \tau_c$  corresponding to  $\max\{\beta_*, \beta_{21}\} = \beta_{21}$  as in Fig. 4. The global maximum entropy state is the asymmetric (mixed) dipole for  $|\Gamma| < \Gamma'_{21}(E) \equiv \sqrt{2E\Lambda'_{21}}$  and the direct monopole for  $|\Gamma| > \Gamma'_{21}(E)$ . There are two second order phase transitions marked by the discontinuity of  $\frac{\partial\alpha}{\partial\Gamma}(\Gamma)$  at  $\Gamma = \pm\Gamma'_{21}(E)$ .

<sup>9</sup> In fact, it is more convenient to plot  $\beta$  as a function of the inverse of the energy  $1/E$  as in Fig. 1 since the interesting bifurcations occurs for large values of the energy.

### 5.6.3 Phase diagram

The phase diagram in the  $(\tau, \Lambda)$  plane, including the metastable states, is plotted in Fig. 5. Depending on the values of  $\Lambda$  and  $\tau$  (and depending on the history of the system in the zone of metastability), the maximum entropy state is a dipole (D), a monopole (MP) or a monopole (MN). If we fix the circulation  $\Gamma$ , we obtain the phase diagram in the  $(\tau, E)$  plane. For  $\Gamma \neq 0$ , it shows the appearance of a second order phase transition in  $\beta(E)$  for  $\tau > \tau_c$  (for  $\Gamma = 0$  there is no phase transition). If we fix the energy  $E$ , we obtain the phase diagram in the  $(\tau, \Gamma)$  plane. As noted by Venaille & Bouchet [40], the point  $(\Gamma = 0, \tau = \tau_c)$  is a bicritical point marking the change from a first order to two second order phase transitions in  $\alpha(\Gamma)$ .

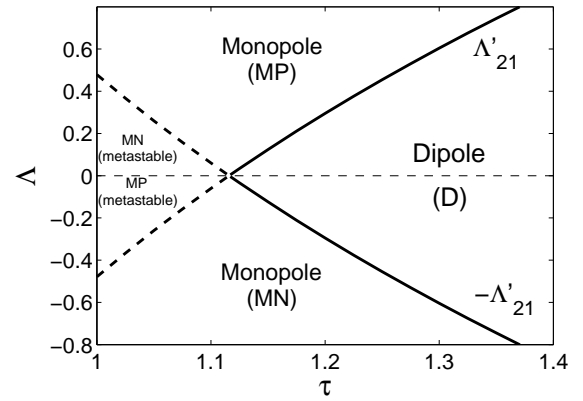


**Fig. 5.** Phase diagram in the  $(\tau, \Lambda)$  plane showing the domain of stability of the direct monopoles and dipoles. We have indicated by a dashed line the domain of metastability of the reversed monopoles.

*Remark:* for illustration, we have described the phase transitions in the case of a rectangular domain and for the Laplacian operator. The generalization to an arbitrary domain and a linear operator  $L$  is straightforward. In that case  $\beta_{21}$  is replaced by  $\beta'_1$  (the first eigenvalue of  $L$  with zero mean) and  $\beta_{11}$  is replaced by  $\beta''_1$  (the first eigenvalue of  $L$  with non zero mean).

## 6 Relaxation towards minimum entropy states

We shall now illustrate numerically the phase transitions discussed previously using the relaxation equations introduced in Appendix D. These relaxation equations can serve as numerical algorithms to compute maximum entropy states or minimum entropy states with relevant constraints. Their study is also interesting in its own right since these equations constitute non trivial dynamical systems leading to rich bifurcations. Although these relaxation equations do not provide a parametrization of 2D

turbulence (we have no rigorous argument for that), they may however give an idea of the true evolution of the flow towards equilibrium. In that respect, it would be interesting to compare these relaxation equations with large eddy simulations (LES) of 2D turbulence. This will, however, not be attempted in the present paper.

### 6.1 Relaxation equations

We shall numerically solve the relaxation equation of Sec. D.3. For simplicity, we shall ignore the advective term since we are just interested in describing the bifurcations between the different equilibrium states. Then, by a proper rescaling of time, we can take  $D = 1$  without loss of generality. The relaxation equation (154) becomes

$$\frac{\partial \omega}{\partial t} = -(\omega + \beta(t)\psi + \alpha(t)), \quad (88)$$

with the boundary condition  $\omega = -\alpha(t)$  on the edge of the domain. The Lagrange multipliers  $\beta(t)$  and  $\alpha(t)$  evolve in time according to Eqs. (155) and (156) in order to conserve the circulation and the energy. This leads to

$$\beta(t) = \frac{\Gamma \langle \psi \rangle - 2E}{\langle \psi^2 \rangle - \langle \psi \rangle^2}, \quad (89)$$

$$\alpha(t) = -\frac{\Gamma \langle \psi^2 \rangle - 2E \langle \psi \rangle}{\langle \psi^2 \rangle - \langle \psi \rangle^2}. \quad (90)$$

The rate of increase of entropy (neg-entropy) is

$$\dot{S} = \int (\omega + \beta\psi + \alpha)^2 d\mathbf{r} \geq 0. \quad (91)$$

Therefore, the relaxation equation (88) with the constraints (89) and (90) relaxes towards the maximum entropy state at fixed circulation and energy. Saddle points of entropy are linearly unstable to some perturbations (in particular those described in Sec. 5.4).

### 6.2 Geometry induced phase transitions and persistence of unstable states

We first consider the case of a square domain ( $\tau = 1 < \tau_c$ ) and take  $\Gamma = 0$ . For these values of parameters, the relaxation equation (88) admits an infinite number of steady states that are the solutions of Eq. (61). However, the only stable solution is the monopole with inverse temperature  $\beta_*$ . It is the maximum entropy state at fixed circulation and energy. In fact, for  $\Gamma = 0$ , this solution is degenerate since the monopoles (MP) and (MN) have the same entropy.

Let us confront these theoretical results to a direct numerical simulation of Eq. (88). Starting from a generic initial condition (made of Gaussian peaks with positive and negative vorticity symmetrically distributed in the domain to assure  $\Gamma = 0$ ), we numerically find that the

system spontaneously relaxes towards the dipole and remains in that state for a long time (see Fig. 6) although this state is predicted to be unstable (see Sec. 5.3). This simple numerical experiment shows that unstable states can be long-lived. In fact, the dipole is a saddle point of entropy so that it is unstable only for very specific perturbations. If these perturbations are not generated spontaneously during the relaxation process, the system can remain frozen in a saddle point for a long time. Another reason why the dipole has a long lifetime is due to the fact that the entropies of the monopole (stable) and dipole (unstable) are very close for  $\Gamma = 0$  since  $\beta_* \approx -46.5$  and  $\beta_{21} \approx -49.3$ . To check that the dipole is really unstable, we have introduced *by hands* (see the arrow in Fig. 6) an optimal perturbation of the form  $\delta\omega = 1 - \beta_*\phi_*$  (see Sec. 5.4). In that case, the dipole is immediately destabilized and the system quickly relaxes towards the monopole which is the maximum entropy state in that case. In the case shown in Fig. 6, we obtain a monopole (MP). If we introduce an optimal perturbation with the opposite sign, we get the monopole (MN). If we do not introduce any perturbation by hand and just let the system evolve with the numerical noise, the dipole finally destabilizes but this takes a long time (not shown) of the order  $t \sim 400$ .

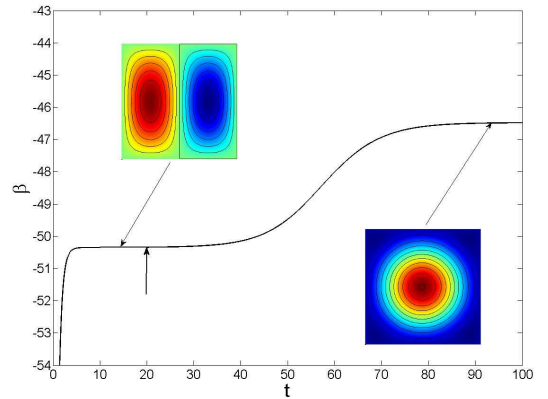


**Fig. 6.** Starting from a generic initial condition with  $\Gamma = 0$  in a square domain, the system relaxes towards a dipole (first plateau) although this solution is unstable (saddle point). At  $t = 20$  (see arrow), an optimal perturbation is applied to the dipole which quickly destabilizes in a stable monopole (second plateau). In the absence of optimal perturbation, the system can remain frozen in the dipole for a long time.

We now consider a rectangular domain with aspect ratio  $\tau = 2 > \tau_c$  and again take  $\Gamma = 0$ . In that case, the maximum entropy state at fixed circulation and energy is the dipole and the monopole is unstable (saddle point).

Starting from a generic initial condition, the system spontaneously relaxes towards the dipole and remains in this state even if very large perturbations are applied (not shown). By contrast, if we start from the monopole, we numerically observe that the system remains in that state for a very long time although this state is unstable (see Sec. 5.3). If we apply *by hands* (see the arrow in Fig. 7) an



optimal perturbation of the form  $\delta\omega = \psi_{21}$  (see Sec. 5.4), the monopole is immediately destabilized and the system quickly evolves towards the dipole (Fig. 7) which is the maximum entropy state in that case. In the absence of applied perturbation, we have not observed the destabilization of the monopole on the timescale achieved in the numerical experiment (if we add the advection term, the dipole is formed on a time of the order  $t \sim 400$ ).

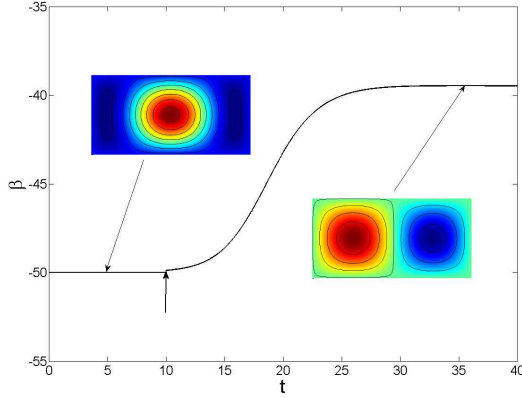


**Fig. 7.** Starting from a monopole with  $\Gamma = 0$  in a rectangular domain ( $\tau > \tau_c$ ), the system remains in that state for a long time (first plateau) although this state is unstable (saddle point). At  $t = 10$  (see arrow), an optimal perturbation is applied to the monopole which quickly relaxes towards a dipole (second plateau). In the absence of optimal perturbation, the system can remain frozen in the monopole state for a long time.

In conclusion, this numerical study reveals that even unstable states (saddle points of entropy) can be naturally selected by the system and persist for a long time. Indeed, these states are destabilized by a very particular type of perturbations (that we call optimal) and such perturbations may not be necessarily generated by the internal dynamics of the system. This suggests that the system can be frozen for a long time in a quasi stationary state (QSS) that is not necessarily a stable or metastable steady state of the 2D Euler equation. It can even be an unstable saddle point! This observation has been made on the basis of the relaxation equations that are constructed so as to relax towards a maximum entropy state. However, the same phenomenon could appear for real flows described by the Euler or Navier-Stokes equations in numerical simulations and laboratory experiments. This could be interesting to study in more detail.

### 6.3 Metastability and hysteresis

We shall now describe the hysteretic cycle predicted by statistical mechanics (based on the neg-entropy) in a domain with aspect ratio  $\tau < \tau_c$ . In Fig. 8, we plot the entropy  $S/E$  as a function of the control parameter  $\Lambda$ . We shall assume that the energy  $E$  is fixed so that  $\Lambda$  basically represents the circulation  $\Gamma$ . The hysteresis is

due to the presence of metastable states (local entropy maxima) when  $-\Lambda'_{21} < \Lambda < \Lambda'_{21}$ . For  $0 < \Lambda < \Lambda'_{12}$ , the global maximum entropy state is the direct monopole (MP) while the reversed monopole (MN) is metastable. For  $-\Lambda'_{12} < \Lambda < 0$ , the global maximum entropy state is the direct monopole (MN) while the reversed monopole (MP) is metastable. Depending on how it has been prepared initially, the system can be found in the stable or metastable state.

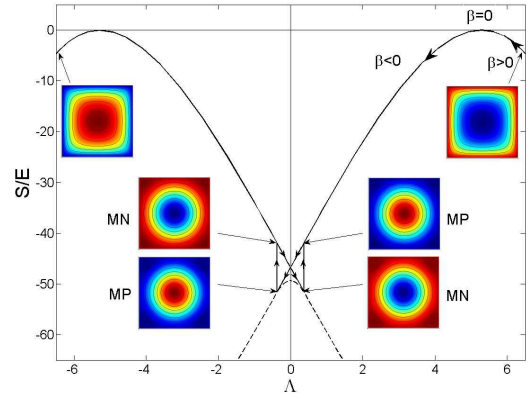


**Fig. 8.**  $S/E$  ratio as a function of  $\Lambda$  in a square domain.

We start from a state with large  $\Lambda$  corresponding to positive temperature ( $\beta > 0$ ). In that case, the positive vorticity has the tendency to accumulate on the boundary of the domain. If we reduce  $\Lambda$ , we enter in the region of negative temperature states ( $\beta < 0$ ). In that case, the positive vorticity has the tendency to accumulate at the center of the domain. For  $\Lambda > 0$ , the (global) maximum entropy state is the monopole (MP). For  $\Lambda = 0$ , we expect a first order phase transition from the monopole (MP) to the monopole (MN) (see Sec. 5.3) marked by the discontinuity of the chemical potential  $\alpha$  (while  $\beta$  and  $S$  are still continuous). In fact, for  $-\Lambda'_{12} < \Lambda \leq 0$ , the monopole (MP) is metastable and robust so that the system remains on this branch. Therefore, in practice, the first order phase transition does not take place. However, for  $\Lambda < -\Lambda'_{12}$ , the branch of monopoles (MP) becomes unstable and the system jumps to the branch of direct monopoles (MN) which correspond to global entropy maxima. This is marked by a discontinuity of entropy (zeroth order phase transition). If we decrease  $\Lambda$  sufficiently, we enter in the region of positive temperature states ( $\beta > 0$ ). In that case, the negative vorticity has the tendency to accumulate on the boundary of the domain. If we now increase  $\Lambda$  the system follows the branch of monopoles (MN) which is stable for  $\Lambda < 0$  and metastable for  $0 < \Lambda < \Lambda'_{12}$ . Again, the first order phase transition at  $\Gamma = 0$  does not take place. For  $\Lambda > \Lambda'_{12}$ , the branch of monopoles (MN) becomes unstable and the system jumps to the branch of direct monopoles (MP) which correspond to global entropy maxima. We have thus followed an hysteretic cycle as illustrated in Figs. 8 and 9.

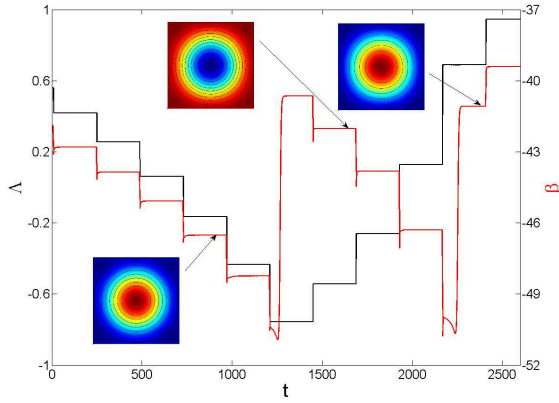


**Fig. 9.** Hysteretic cycle in a square domain, obtained by numerical integration of Eq. (88). We have represented  $\Lambda$  (black) and  $\beta$  (red) as a function of time. Starting from a stable state with  $\Lambda \in [0; \Lambda'_{21}]$  (MP), the system is regularly perturbed: at  $t = 10, 250, 490, 730, 970, 1210$ , we add to the vorticity distribution the sum of a negative Gaussian peak and an eigenmode  $0.1\psi_{21}$ , and let the system relax. The effect of the Gaussian peak is to decrease  $\Lambda$ , while the eigenmode destabilizes the unstable states. For  $0 < \Lambda < \Lambda'_{21}$  we follow the stable branch (MP) of Fig. 8 and for  $-\Lambda'_{21} < \Lambda < 0$ , we follow the metastable branch (MP). For  $\Lambda < -\Lambda'_{21}$ , the metastable solutions (MP) no longer exist, and the system jumps to the upper branch (MN) of Fig. 8. At  $t = 1450, 1690, 1930, 2170, 2410$ , we add to the vorticity distribution the sum of a positive Gaussian peak and an eigenmode  $0.05\psi_{21}$ . The value of  $\Lambda$  is then increased, and we follow the stable branch (MN) for  $\Lambda \in [-\Lambda'_{21}; 0]$  and the metastable branch (MN) for  $\Lambda \in [0; \Lambda'_{21}]$ . When  $\Lambda > \Lambda'_{21}$ , the metastable solutions (MN) no longer exist, and the system jumps to the upper branch (MP) of Fig. 8.

#### 6.4 Bifurcations in the presence of a noise

For  $\Gamma = 0$  in a square domain, the monopoles (MP) and (MN) are stable and have the same entropy but remain quite distinct states (with opposite velocity). This corresponds to a parity breaking for the final organization of the system [26]. In the presence of forcing, we expect to observe random transitions between these two solutions<sup>10</sup> similar to those observed experimentally by Sommeria [49] for 2D turbulence forced at small scale in a square box. Indeed, we are in a situation similar to the case of a bistable system. To observe such transitions, one possibility is to introduce a stochastic noise in the relaxation equation (88). Unfortunately, for a simple white noise, we did not observe any transition and we have not been able to find the properties of forcing that allow such transitions to appear. This may be due to the high entropic barrier created by the unstable (dipole) solution. Therefore, in order to illustrate the main idea, we shall introduce a simple effective model.

The relevant order parameter is the chemical potential  $\alpha$  which takes the values  $\pm\alpha_0$  for the (stable) monopoles (MP) and (MN) and the value  $\alpha = 0$  for the (unsta-

ble) dipole (see Fig. 3). We shall now introduce an entropic function  $S(\alpha)$  modeled by a symmetric function with three bumps (two maxima and one minimum). Since we know the entropy (by unit of energy) of the monopoles  $S_{monopoles} = \beta_*$  and the entropy of the dipole  $S_{dipole} = \beta_{21}$ , we find that

$$S(\alpha) = (\beta_{21} - \beta_*) \left[ 1 - \left( \frac{\alpha}{\alpha_0} \right)^2 \right]^2 + \beta_*. \quad (92)$$

When a forcing is present, we can propose that  $\alpha$  becomes a stochastic variable described by a Langevin equation of the form

$$\frac{d\alpha}{dt} = \mu S'(\alpha) + \sqrt{2D}\eta(t), \quad (93)$$

where  $\eta(t)$  is a white noise. In the absence of forcing, Eq. (93) relaxes towards one maximum of  $S(\alpha)$ , the monopole (MP) or the monopole (MN), and stay there permanently. In the presence of forcing, Eq. (93) describes random transitions between these two states (see Fig. 10). This is the classical bistable system that has been studied at length in statistical mechanics and Brownian theory [50].

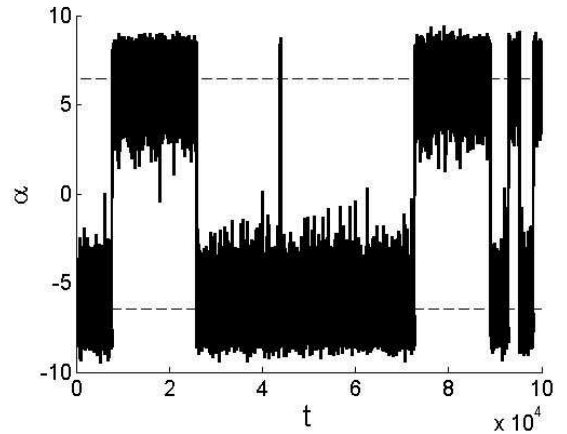


**Fig. 10.** Solution of the stochastic equation (93) for  $\mu = 1.0$  and  $D = 1.25$  showing random transitions between the monopoles (MP) and (MN). The dipole is always unstable.

Random transitions have been observed in various physical systems in fluid mechanics (see, e.g., [49, 51, 45] and references therein). In the present study, we have considered random transitions between a monopole (MP) and a reversed monopole (MN). They are associated with the first order phase transition that takes place in a square domain when the QSS has a linear  $\omega - \psi$  relationship. It would be interesting to see if they can be obtained directly from the forced Navier-Stokes equations in situations where the  $\omega - \psi$  relationship is close to linear. Random transitions between a unidirectional flow and a dipole have been obtained recently by Bouchet & Simonnet [45] by solving numerically the forced Navier-Stokes equations in periodic domain. However, the situation is different (and more complex) because these two states are

<sup>10</sup> This idea was initially proposed in [26].

characterized by different  $\omega - \psi$  relationships. Indeed, the forcing can change the shape of  $\omega(\psi)$ . In the situation that we consider, the shape of  $\omega(\psi)$  remains the same (linear) but the equation  $\Delta\psi = -\omega(\psi)$  determining the QSS can admit two stable solutions (MP) and (MN). This situation is closer to that of a bistable system and would be interesting to study numerically.

## 7 Conclusion

In this paper, we have studied the maximization of the Miller-Robert-Sommeria entropy  $S_{MRS}$  at fixed energy  $E$ , circulation  $\Gamma$  and microscopic enstrophy  $\Gamma_2^{f.g.}$  and proved the equivalence with the minimization of the macroscopic enstrophy  $\Gamma_2^{c.g.}$  at fixed energy  $E$  and circulation  $\Gamma$ . This provides a justification of the minimum enstrophy principle from statistical theory when only the microscopic enstrophy is conserved among all the Casimir invariants. We have suggested that relevant constraints (such as the microscopic enstrophy) are selected by the properties of forcing and dissipation. Our simplified thermodynamic approach leads to a mean flow characterized by a linear  $\bar{\omega} - \psi$  relationship and Gaussian fluctuations around it. Such states can be relevant to describe certain oceanic flows [6, 7, 8, 9, 10, 11, 12, 13, 14, 15, 16, 17, 18, 19, 20]. More general flows with nonlinear  $\bar{\omega} - \psi$  relationships (and more general fluctuations) can be constructed in principle by keeping additional Casimir constraints apart from the microscopic enstrophy.

We have studied the minimization of enstrophy at fixed energy and circulation and analyzed the corresponding phase transitions with the approach of Chavanis & Sommeria [26]. We have discussed the link with the approach of Venaille & Bouchet [40]. We have proposed relaxation equations to solve this minimization problem (see [34] for generalizations) and used them to illustrate the phase transitions.

One interesting result of the simulations is the observation that saddle points of entropy can be relevant in the dynamics. Indeed, these states are unstable only for particular perturbations that are not necessarily generated spontaneously by the system. As a result, they can be long-lived and robust. This observation may have interesting application in the case of von Kármán flows since it is found that Beltrami states are saddle points of energy at fixed helicity, not energy minima [37]. Still, it is observed experimentally [35, 36] that they are long-lived and robust.

We have also discussed in detail the metastable states that were not considered in the study of Venaille & Bouchet [40]. For long-range interactions, metastable states (local entropy maxima) are long-lived and they are as much important as fully stable states (global entropy maxima). Interestingly, these metastable states have negative specific heats leading to a form of ensemble inequivalence between the microcanonical and canonical ensembles (while these ensembles are equivalent at the level of fully stable states [40]). These metastable states can lead

to an hysteresis and to random transitions between direct monopoles and reversed monopoles. Such transitions can also arise in more realistic fluid systems and can have some importance in oceanography and meteorology [49, 51, 45].

A last remark may be in order. The MRS statistical theory of the 2D Euler equation, which is the most basic and the most rigorous, takes into account an infinite number of constraints. When applied to real flows, this is clearly unphysical and this leads to practical difficulties. It has been a subject of intense debate in the last 20 years to find a practical way to deal with the constraints. Different approaches have been proposed: some consider a point vortex approximation where only the energy and the number of vortices in each species matter [22], some consider since the start only a finite number of inviscid constraints [18, 19, 20], some consider a strong mixing (or low energy) limit of the MRS statistical theory which makes a hierarchy among the Casimir constraints [26], and some model the vorticity fluctuations by a prior distribution [29, 30, 31]. In our recent works [34, 48], including the present one, we have not tried to determine which approach, if any, is the “best”. For the moment, we just present different ways to deal with the constraints and systematically study the corresponding variational principles. We have also extended these variational principles to 3D axisymmetric flows [37]. These variational principles have a long history in 2D turbulence and MHD and one virtue of our papers is to put several variational principles in correspondence. The determination of the “best” approach is still a matter of debate and research.

## A Equivalence between (29) and (54)

In Sec. 4, we have shown the equivalence of (16) and (46) for global maximization. In this Appendix, we show the equivalence of (16) and (46) for local maximization, i.e.  $\rho(\mathbf{r}, \sigma)$  is a (local) maximum of  $S[\rho]$  at fixed  $E$ ,  $\Gamma$ ,  $\Gamma_2^{f.g.}$  and normalization if, and only if, the corresponding coarse-grained vorticity  $\bar{\omega}(\mathbf{r})$  is a (local) minimum of  $\Gamma_2^{c.g.}[\bar{\omega}]$  at fixed  $E$  and  $\Gamma$ . To that purpose, we show the equivalence between the stability criteria (29) and (54). We use a general method similar to the one used in [48, 52, 53] in related problems.

We shall determine the optimal perturbation  $\delta\rho_*(\mathbf{r}, \sigma)$  that maximizes  $\delta^2 J[\delta\rho]$  given by Eq. (29) with the constraints  $\delta\bar{\omega} = \int \delta\rho\sigma d\sigma$ ,  $\delta\Gamma_2^{f.g.} = \int \delta\rho\sigma^2 d\sigma d\mathbf{r} = 0$  and  $\int \delta\rho d\sigma = 0$ , where  $\delta\bar{\omega}(\mathbf{r})$  is prescribed (it is only ascribed to conserve circulation and energy at first order). Since the specification of  $\delta\bar{\omega}$  determines  $\delta\psi$ , hence the second integral in Eq. (29), we can write the variational problem in the form

$$\delta \left( -\frac{1}{2} \int \frac{(\delta\rho)^2}{\rho} d\mathbf{r} d\sigma \right) - \int \lambda(\mathbf{r}) \delta \left( \int \delta\rho\sigma d\sigma \right) d\mathbf{r} - \mu \delta \left( \int \delta\rho\sigma^2 d\sigma d\mathbf{r} \right) - \int \zeta(\mathbf{r}) \delta \left( \int \delta\rho d\sigma \right) d\mathbf{r} = 0, \quad (94)$$

where  $\lambda(\mathbf{r})$ ,  $\mu$  and  $\zeta(\mathbf{r})$  are Lagrange multipliers. This gives

$$\delta\rho_*(\mathbf{r}, \sigma) = -\rho(\mathbf{r}, \sigma)(\mu\sigma^2 + \lambda(\mathbf{r})\sigma + \zeta(\mathbf{r})), \quad (95)$$

and it is a global maximum of  $\delta^2 J[\delta\rho]$  with the previous constraints since  $\delta^2(\delta^2 J) = -\int \frac{(\delta(\delta\rho))^2}{2\rho} d\mathbf{r}d\sigma < 0$  (the constraints are linear in  $\delta\rho$  so their second variations vanish). The Lagrange multipliers are determined from the above-mentioned constraints. The constraints  $\int \delta\rho d\sigma = 0$  and  $\delta\bar{\omega} = \int \delta\rho\sigma d\sigma$  lead to

$$\zeta(\mathbf{r}) + \lambda(\mathbf{r})\bar{\omega}(\mathbf{r}) + \mu\bar{\omega}^2(\mathbf{r}) = 0, \quad (96)$$

$$\zeta(\mathbf{r})\bar{\omega}(\mathbf{r}) + \lambda(\mathbf{r})\bar{\omega}^2(\mathbf{r}) + \mu\bar{\omega}^3(\mathbf{r}) = -\delta\bar{\omega}(\mathbf{r}). \quad (97)$$

Now, the state  $\rho(\mathbf{r}, \sigma)$  corresponds to the gaussian distribution (27). Therefore, we have the well-known relations  $\bar{\omega}^2(\mathbf{r}) = \bar{\omega}^2(\mathbf{r}) + \omega_2$  and  $\bar{\omega}^3(\mathbf{r}) = \bar{\omega}^3(\mathbf{r}) + 3\bar{\omega}(\mathbf{r})\omega_2$  where  $\omega_2 = \Omega_2$  is uniform. Substituting these relations in Eqs. (96) and (97), and solving for  $\lambda(\mathbf{r})$  and  $\zeta(\mathbf{r})$ , we obtain

$$\lambda(\mathbf{r}) = -\frac{\delta\bar{\omega}(\mathbf{r})}{\omega_2} - 2\mu\bar{\omega}(\mathbf{r}), \quad (98)$$

$$\zeta(\mathbf{r}) = \frac{\bar{\omega}(\mathbf{r})}{\omega_2}\delta\bar{\omega}(\mathbf{r}) + \mu\bar{\omega}^2(\mathbf{r}) - \mu\omega_2. \quad (99)$$

Therefore, the optimal perturbation (95) can be rewritten

$$\delta\rho_* = -\rho \left[ -\frac{\delta\bar{\omega}}{\omega_2}(\sigma - \bar{\omega}) + \mu \{(\sigma - \bar{\omega})^2 - \omega_2\} \right]. \quad (100)$$

The Lagrange multiplier  $\mu$  is determined by substituting this expression in the constraint  $\int \delta\rho\sigma^2 d\mathbf{r}d\sigma = 0$ . Using the well-known identity  $\bar{\omega}^4(\mathbf{r}) = \bar{\omega}^4(\mathbf{r}) + 6\omega_2\bar{\omega}^2(\mathbf{r}) + 3\omega_2^2$  valid for a gaussian distribution, we obtain after some simplifications

$$\mu = \frac{\int \bar{\omega}\delta\bar{\omega} d\mathbf{r}}{\omega_2^2}. \quad (101)$$

Therefore, the optimal perturbation (95) is given by Eq. (100) with Eq. (101). Since this perturbations maximizes  $\delta^2 J[\delta\rho]$  with the above-mentioned constraints, we have  $\delta^2 J[\delta\rho] \leq \delta^2 J[\delta\rho_*]$ . Explicating  $\delta^2 J[\delta\rho_*]$  using Eqs. (100) and (101), we obtain after simple calculations

$$\delta^2 J[\delta\rho] \leq -\frac{1}{2\omega_2} \int (\delta\bar{\omega})^2 d\mathbf{r} - \frac{1}{\omega_2^2} \left( \int \bar{\omega}\delta\bar{\omega} d\mathbf{r} \right)^2 - \frac{1}{2}\beta \int \delta\bar{\omega}\delta\psi d\mathbf{r}. \quad (102)$$

The r.h.s. returns the functional appearing in Eq. (43). We have already explained in Sec. 4.2 that for the class of perturbations that we consider ( $\delta\Gamma = \delta E = 0$ ) the second integral vanishes. Therefore, the foregoing inequality can be rewritten

$$\delta^2 J[\delta\rho] \leq -\frac{1}{2\omega_2} \int (\delta\bar{\omega})^2 d\mathbf{r} - \frac{1}{2}\beta \int \delta\bar{\omega}\delta\psi d\mathbf{r}, \quad (103)$$

where the r.h.s. is precisely the functional appearing in Eq. (54). Furthermore, there is equality in Eq. (103) if

$\delta\rho = \delta\rho_*$ . This proves that the stability criteria (29) and (54) are equivalent. Indeed: (i) if inequality (54) is fulfilled for all perturbations  $\delta\bar{\omega}$  that conserves circulation and energy at first order, then according to Eq. (103), we know that inequality (29) is fulfilled for all perturbation  $\delta\rho$  that conserves circulation, energy, fine-grained enstrophy and normalization at first order; (ii) if there exists a perturbation  $\delta\bar{\omega}_*$  that makes  $\delta^2 J[\delta\bar{\omega}] > 0$ , then the perturbation  $\delta\rho_*$  given by Eq. (100) with Eq. (101) and  $\delta\bar{\omega} = \delta\bar{\omega}_*$  makes  $\delta^2 J[\delta\rho] > 0$ . In conclusion, the stability criteria (29) and (54) are equivalent.

## B Eigenvalues and eigenfunctions of the Laplacian in a rectangular domain

We define the eigenfunctions and eigenvalues of the Laplacian by

$$\Delta\psi_n = \beta_n\psi_n, \quad (104)$$

with  $\psi_n = 0$  on the domain boundary. These eigenfunctions are orthogonal and normalized so that  $\langle\psi_n\psi_m\rangle = \delta_{nm}$ . Since  $-\int (\nabla\psi_n)^2 d\mathbf{r} = \beta_n \int \psi_n^2 d\mathbf{r}$ , we note that  $\beta_n < 0$ . Following Chavanis & Sommeria [26], we distinguish two types of eigenmodes: the odd eigenmodes  $\psi'_n$  such that  $\langle\psi'_n\rangle = 0$  and the even eigenmodes  $\psi''_n$  such that  $\langle\psi''_n\rangle \neq 0$ . We note  $\beta'_n$  and  $\beta''_n$  the corresponding eigenvalues.

In a rectangular domain of unit area whose sides are denoted  $a = \sqrt{\tau}$  and  $b = 1/\sqrt{\tau}$  (where  $\tau = a/b$  is the aspect ratio), the eigenmodes and eigenvalues are

$$\psi_{mn} = 2 \sin(m\pi x/\sqrt{\tau}) \sin(n\pi\sqrt{\tau}y), \quad (105)$$

$$\beta_{mn} = -\pi^2 \left( \frac{m^2}{\tau} + \tau n^2 \right), \quad (106)$$

where the origin of the Cartesian frame is taken at the lower left corner of the domain. The integer  $m \geq 1$  gives the number of vortices along the  $x$ -axis and  $n \geq 1$  the number of vortices along the  $y$ -axis. We have  $\langle\psi_{mn}\rangle = 0$  if  $m$  or  $n$  is even and  $\langle\psi_{mn}\rangle \neq 0$  if  $m$  and  $n$  are odd.

The differential equation (70) can be solved analytically by decomposing the field  $\phi$  on the eigenmodes as  $\phi = \sum_{mn} c_{mn}\psi_{mn}$  and using the identity  $1 = \sum_{mn} \langle\psi_{mn}\rangle\psi_{mn}$ . This yields Eq. (71) from which we obtain

$$\langle\phi\rangle = \sum_{mn} \frac{\langle\psi_{mn}\rangle^2}{\beta - \beta_{mn}}, \quad (107)$$

$$\langle\phi^2\rangle = \sum_{mn} \frac{\langle\psi_{mn}\rangle^2}{(\beta - \beta_{mn})^2} = -\frac{d\langle\phi\rangle}{d\beta}. \quad (108)$$

We note in particular that

$$\langle\phi\rangle - \beta\langle\phi^2\rangle = -\sum_{mn} \frac{\beta_{mn}\langle\psi_{mn}\rangle^2}{(\beta - \beta_{mn})^2} > 0. \quad (109)$$



## C Temporal evolution of the different modes

The relaxation equation (88) can be solved analytically by decomposing the vorticity and the stream function on the eigenmodes of the Laplacian. Using the Poisson equation, we get  $\omega(\mathbf{r}, t) = \sum_n a_n(t) \psi_n(\mathbf{r})$  and  $\psi(\mathbf{r}, t) = \sum_n b_n(t) \psi_n(\mathbf{r})$  with  $b_n(t) = -a_n(t)/\beta_n$ . Substituting these expressions in Eq. (88) and using the identity  $1 = \sum_n \langle \psi_n \rangle \psi_n$ , we obtain the ordinary differential equations

$$\frac{da_n}{dt} + \left(1 - \frac{\beta(t)}{\beta_n}\right) a_n = -\alpha(t) \langle \psi_n \rangle, \quad (110)$$

for all  $n$ . The evolution of the Lagrange multipliers is given by Eqs. (89) and (90) with  $\langle \psi \rangle = \sum_n b_n(t) \langle \psi_n \rangle$  and  $\langle \psi^2 \rangle = \sum_n b_n^2(t)$ . The modes are coupled through the Lagrange multipliers in order to assure the conservation of energy and circulation.

In the grand canonical description in which  $\beta$  and  $\alpha$  are constants, the foregoing differential equation can be integrated straightforwardly, yielding

$$a_n(t) = \left( a_n(0) + \frac{\alpha \langle \psi_n \rangle}{1 - \beta/\beta_n} \right) e^{-(1 - \beta/\beta_n)t} - \frac{\alpha \langle \psi_n \rangle}{1 - \beta/\beta_n}. \quad (111)$$

In that case, a steady state of the relaxation equation is stable iff  $\beta > \beta'_1$  where  $\beta'_1$  is the largest eigenvalue of the Laplacian. The condition  $\beta > \beta'_1$  is a necessary and sufficient condition for the steady state to be a global maximum of the grand potential  $G = S - \beta E - \alpha \Gamma$ . That functional is related to the Arnol'd energy-Casimir functional [34].

## D Relaxation equations

### D.1 Relaxation equations associated with the maximization problem (16)

In this Appendix, we construct relaxation equations associated with the maximization problem (16) corresponding to the energy-entropy statistical theory. These relaxation equations can serve as a numerical algorithm to solve this constrained maximization problem. In the past, Robert & Sommeria [54] have proposed relaxation equations that conserve all the Casimirs and increase the entropy. Here, we use a different approach because we want to conserve only the microscopic enstrophy (not all the Casimirs). Thus, the form of the relaxation equations will be different. In particular, they will involve a current in the space of vorticity levels  $\sigma$  [34, 48] instead of a current in the space of positions [54].

We construct a set of relaxation equations that increase  $S[\rho]$  while conserving  $E$ ,  $\Gamma$  and  $\Gamma_2^{f.g.}$  using a Maximum Entropy Production Principle. The dynamical equation that we consider can be written as

$$\frac{\partial \rho}{\partial t} + \mathbf{u} \cdot \nabla \rho = -\frac{\partial J}{\partial \sigma}, \quad (112)$$

where  $J$  is an unknown current to be chosen so as to increase  $S[\rho]$  while conserving the constraints. The local normalization  $\int \rho d\sigma = 1$  is satisfied provided that  $J \rightarrow 0$  as  $\sigma \rightarrow \pm\infty$ . Multiplying Eq. (112) by  $\sigma$  and integrating over the levels, we get

$$\frac{\partial \bar{\omega}}{\partial t} + \mathbf{u} \cdot \nabla \bar{\omega} = \int J d\sigma \equiv X. \quad (113)$$

Next, multiplying Eq. (112) by  $\sigma^2$  and integrating over the levels, we obtain

$$\frac{\partial \bar{\omega}^2}{\partial t} + \mathbf{u} \cdot \nabla \bar{\omega}^2 = 2 \int J \sigma d\sigma. \quad (114)$$

From Eqs. (113) and (114), we find that

$$\frac{\partial \omega_2}{\partial t} + \mathbf{u} \cdot \nabla \omega_2 = 2 \int J (\sigma - \bar{\omega}) d\sigma. \quad (115)$$

Using Eq. (112), the time variations of  $S[\rho]$  are given by

$$\dot{S} = - \int \frac{J}{\rho} \frac{\partial \rho}{\partial \sigma} d\mathbf{r} d\sigma, \quad (116)$$

and the time variations of  $E$ ,  $\Gamma$ ,  $\Gamma_2^{f.g.}$  are given by

$$\dot{E} = \int J \psi d\mathbf{r} d\sigma = 0, \quad (117)$$

$$\dot{\Gamma} = \int J d\mathbf{r} d\sigma = 0, \quad (118)$$

$$\dot{\Gamma}_2^{f.g.} = 2 \int J \sigma d\mathbf{r} d\sigma = 0. \quad (119)$$

Following the Maximum Entropy Production Principle, we maximize  $\dot{S}$  with  $\dot{E} = \dot{\Gamma} = \dot{\Gamma}_2^{f.g.} = 0$  and the additional constraint

$$\int \frac{J^2}{2\rho} d\sigma \leq C(\mathbf{r}, t), \quad (120)$$

putting some physical bound on the diffusion current. The variational principle can be written in the form

$$\delta \dot{S} - \beta(t) \delta \dot{E} - \alpha(t) \delta \dot{\Gamma} - \alpha_2(t) \delta \dot{\Gamma}_2^{f.g.} - \int \frac{1}{D(\mathbf{r}, t)} \delta \left( \int \frac{J^2}{2\rho} d\sigma \right) d\mathbf{r} = 0, \quad (121)$$

where  $\beta(t)$ ,  $\alpha(t)$ ,  $\alpha_2(t)$  and  $D(\mathbf{r}, t)$  are time dependent Lagrange multipliers associated with the constraints. This leads to the following optimal current

$$J = -D \left[ \frac{\partial \rho}{\partial \sigma} + \rho (\beta(t) \psi + \alpha(t) + 2\alpha_2(t) \sigma) \right]. \quad (122)$$

Therefore, the relaxation equation for the vorticity distribution is

$$\begin{aligned} \frac{\partial \rho}{\partial t} + \mathbf{u} \cdot \nabla \rho \\ = \frac{\partial}{\partial \sigma} \left\{ D \left[ \frac{\partial \rho}{\partial \sigma} + \rho (\beta(t) \psi + \alpha(t) + 2\alpha_2(t) \sigma) \right] \right\}. \end{aligned} \quad (123)$$

Integrating Eq. (122) over  $\sigma$ , we obtain

$$X = -D(\beta(t)\psi + \alpha(t) + 2\alpha_2(t)\bar{\omega}). \quad (124)$$

Inserting Eq. (124) into Eq. (113) leads to the following relaxation equation for the mean flow

$$\frac{\partial \bar{\omega}}{\partial t} + \mathbf{u} \cdot \nabla \bar{\omega} = -D(\beta(t)\psi + \alpha(t) + 2\alpha_2(t)\bar{\omega}). \quad (125)$$

For the boundary condition, we shall take  $\beta(t)\psi + \alpha(t) + 2\alpha_2(t)\bar{\omega} = 0$  on the domain boundary so as to be consistent with the equilibrium state where this quantity vanishes in the whole domain. Since  $\psi = 0$  on the boundary, we finally get  $\bar{\omega} = -\alpha(t)/(2\alpha_2(t))$  on the domain boundary. A relaxation equation can also be written for the centered variance  $\omega_2$ . Using Eqs. (122) and (115), we obtain

$$\frac{\partial \omega_2}{\partial t} + \mathbf{u} \cdot \nabla \omega_2 = 2D(1 - 2\alpha_2(t)\omega_2). \quad (126)$$

Finally, in Eqs. (123), (125) and (126), the Lagrange multipliers evolve so as to satisfy the constraints. Substituting Eq. (122) in Eqs. (117), (118) and (119), we obtain the algebraic equations

$$\langle \psi^2 \rangle \beta(t) + \langle \psi \rangle \alpha(t) + 4E\alpha_2(t) = 0, \quad (127)$$

$$\langle \psi \rangle \beta(t) + \alpha(t) + 2\Gamma\alpha_2(t) = 0, \quad (128)$$

$$2E\beta(t) + \Gamma\alpha(t) + 2\Gamma_2^{f.g.}\alpha_2(t) = 1. \quad (129)$$

where  $\langle X \rangle = \int X d\mathbf{r}$ . Substituting  $\partial\rho/\partial\sigma$  taken from Eq. (122) in Eq. (116) and using the constraints (117)-(119), we easily obtain

$$\dot{S} = \int \frac{J^2}{D\rho} d\mathbf{r} d\sigma, \quad (130)$$

so that  $\dot{S} \geq 0$  provided that  $D$  is positive. On the other hand  $\dot{S} = 0$  iff  $J = 0$  leading to the Gibbs state (23). From Lyapunov's direct method, we conclude that these relaxation equations tend to a maximum of entropy at fixed energy, circulation and microscopic enstrophy. Note that during the relaxation process, the distribution of vorticity is not Gaussian but changes with time according to Eq. (123). The vorticity distribution is Gaussian only at equilibrium. Therefore, these relaxation equations describe not only the evolution of the mean flow according to Eq. (125) but also the evolution of the full vorticity distribution according to Eq. (123). We stress, however, that these equations are purely phenomenological and that there is no compelling reason why they should give an accurate description of the real dynamics. However, they can be used at least as a numerical algorithm to compute the statistical equilibrium state. Indeed, these equations can only relax towards an entropy maximum at fixed energy, circulation and microscopic enstrophy, not towards a minimum or a saddle point that are linearly unstable with respect to these equations<sup>11</sup>.

<sup>11</sup> In fact, we show in Sec. 6 that the system can remain blocked in an unstable state (saddle point of entropy) if the

## D.2 Relaxation equations associated with the maximization problem (36)

We shall now introduce a set of relaxation equations associated with the maximization problem (36). We write the dynamical equation as

$$\frac{\partial \bar{\omega}}{\partial t} + \mathbf{u} \cdot \nabla \bar{\omega} = X, \quad (131)$$

where  $X$  is an unknown quantity to be chosen so as to increase  $S[\bar{\omega}]$  while conserving  $E$ ,  $\Gamma$  and  $\Gamma_2^{f.g.}$ . The time variations of  $S$  are given by

$$\dot{S} = -\frac{1}{\Omega_2(t)} \int \bar{\omega} X d\mathbf{r}, \quad (132)$$

where  $\Omega_2(t)$  is determined by the constraint on microscopic enstrophy leading to

$$\Omega_2(t) = \Gamma_2^{f.g.} - \int \bar{\omega}^2 d\mathbf{r}, \quad (133)$$

at each time. On the other hand, the time variations of  $E$  and  $\Gamma$  are

$$\dot{E} = \int X \psi d\mathbf{r} = 0, \quad (134)$$

$$\dot{\Gamma} = \int X d\mathbf{r} = 0. \quad (135)$$

Following the Maximum Entropy Production Principle, we maximize  $\dot{S}$  with  $\dot{E} = \dot{\Gamma} = 0$  (the conservation of microscopic enstrophy has been taken into account in Eq. (133)) and the additional constraint

$$\frac{X^2}{2} \leq C(\mathbf{r}, t). \quad (136)$$

The variational principle can be written in the form

$$\delta \dot{S} - \beta(t) \delta \dot{E} - \alpha(t) \delta \dot{\Gamma} - \int \frac{1}{D(\mathbf{r}, t)} \delta \left( \frac{X^2}{2} \right) d\mathbf{r} = 0, \quad (137)$$

and it leads to the optimal quantity

$$X = -D \left( \beta(t)\psi + \alpha(t) + \frac{1}{\Omega_2(t)} \bar{\omega} \right). \quad (138)$$

Inserting Eq. (138) in Eq. (131), we obtain

$$\frac{\partial \bar{\omega}}{\partial t} + \mathbf{u} \cdot \nabla \bar{\omega} = -D \left( \beta(t)\psi + \alpha(t) + \frac{1}{\Omega_2(t)} \bar{\omega} \right), \quad (139)$$

with  $\bar{\omega} = -\alpha(t)\Omega_2(t)$  on the domain boundary. The Lagrange multipliers evolve so as to satisfy the constraints.

dynamics does not spontaneously develop the “dangerous” perturbations that make it unstable. This is because the system is unstable only for some perturbations but not for any perturbation. Therefore, we must keep in mind this property when we use the relaxation equations.

Substituting Eq. (138) in Eqs. (134)-(135) and recalling Eq. (133), we obtain the algebraic equations

$$\Omega_2(t) = \Gamma_2^{f.g.} - \int \bar{\omega}^2 d\mathbf{r}, \quad (140)$$

$$\langle \psi^2 \rangle \beta(t) + \langle \psi \rangle \alpha(t) = -\frac{2E}{\Omega_2(t)}, \quad (141)$$

$$\langle \psi \rangle \beta(t) + \alpha(t) = -\frac{\Gamma}{\Omega_2(t)}. \quad (142)$$

Substituting  $\bar{\omega}$  taken from Eq. (138) in Eq. (132) and using the constraints (134)-(135), we easily obtain

$$\dot{S} = \int \frac{X^2}{D} d\mathbf{r}, \quad (143)$$

so that  $\dot{S} \geq 0$  provided that  $D$  is positive. On the other hand  $\dot{S} = 0$  iff  $X = 0$  leading to the condition of equilibrium (42). From Lyapunov's direct method, we conclude that these relaxation equations tend to a maximum of entropy at fixed energy, circulation and microscopic enstrophy.

The relaxation equation (139) is similar to Eq. (125) but the constraints determining the evolution of the Lagrange multipliers are different. More precisely, Eqs. (141) and (142) are equivalent to Eqs. (128) and (129) but Eq. (127) has been replaced by Eq. (133). Indeed, in the present approach, the vorticity distribution is always Gaussian during the dynamical evolution. It is given by Eq. (32) at any time, i.e.

$$\rho(\mathbf{r}, \sigma, t) = \frac{1}{\sqrt{2\pi\Omega_2(t)}} e^{-\frac{(\sigma - \bar{\omega}(\mathbf{r}, t))^2}{2\Omega_2(t)}}. \quad (144)$$

By contrast, in the approach of Sec. D.1, the vorticity distribution changes with time. Therefore, the dynamical evolution is different. However, in the two approaches, the equilibrium state is the same, i.e. it solves the maximization problem (16). This is sufficient if we use these relaxation equations as numerical algorithms to compute the maximum entropy state.

*Remark:* Using Eqs. (131)-(132), it is easy to show that  $\dot{\Gamma}_2^{c.g.} = -2\Omega_2(t)\dot{S}$  so that  $\dot{\Gamma}_2^{c.g.} \leq 0$  since  $\Omega_2(t) \geq 0$  (by Schwartz inequality). Therefore, the macroscopic enstrophy decreases monotonically through the relaxation equations. This is to be expected since the maximization problem (36) is equivalent to the minimization of the macroscopic enstrophy at fixed energy and circulation (see Sec. 4.3).

*Alternative relaxation equation:* writing the r.h.s. of Eq. (131) in the form of the divergence of a current in order to conserve the circulation, and using a MEPP, we obtain a relaxation of the form [34]:

$$\frac{\partial \bar{\omega}}{\partial t} + \mathbf{u} \cdot \nabla \bar{\omega} = \nabla \cdot \left[ D \left( \frac{1}{\Omega_2(t)} \nabla \bar{\omega} + \beta(t) \nabla \psi \right) \right], \quad (145)$$

where  $\Omega_2(t)$  is given by Eq. (140) and  $\beta(t)$  by

$$\beta(t) = \frac{-\int D \nabla \bar{\omega} \cdot \nabla \psi d\mathbf{r}}{\Omega_2(t) \int D (\nabla \psi)^2 d\mathbf{r}}. \quad (146)$$

The boundary conditions are  $(\frac{1}{\Omega_2(t)} \nabla \bar{\omega} + \beta(t) \nabla \psi) \cdot \mathbf{n} = 0$  on the domain boundary. This relaxation equation satisfies the same general properties as Eq. (139).

### D.3 Relaxation equations associated with the maximization problem (46)

We shall introduce a set of relaxation equations associated with the maximization problem (46). We write the dynamical equation as

$$\frac{\partial \bar{\omega}}{\partial t} + \mathbf{u} \cdot \nabla \bar{\omega} = X, \quad (147)$$

where  $X$  is an unknown quantity to be chosen so as to increase  $S[\bar{\omega}]$  while conserving  $E$  and  $\Gamma$ . The time variations of  $S$  are given by

$$\dot{S} = - \int \bar{\omega} X d\mathbf{r}. \quad (148)$$

On the other hand, the time variations of  $E$  and  $\Gamma$  are

$$\dot{E} = \int X \psi d\mathbf{r} = 0, \quad (149)$$

$$\dot{\Gamma} = \int X d\mathbf{r} = 0. \quad (150)$$

Following the Maximum Entropy Production Principle, we maximize  $\dot{S}$  with  $\dot{E} = \dot{\Gamma} = 0$  and the additional constraint

$$\frac{X^2}{2} \leq C(\mathbf{r}, t). \quad (151)$$

The variational principle can be written in the form

$$\delta \dot{S} - \beta(t) \delta \dot{E} - \alpha(t) \delta \dot{\Gamma} - \int \frac{1}{D(\mathbf{r}, t)} \delta \left( \frac{X^2}{2} \right) d\mathbf{r} = 0, \quad (152)$$

and we obtain

$$X = -D(\beta(t)\psi + \alpha(t) + \bar{\omega}). \quad (153)$$

Substituting Eq. (153) in Eq. (147), we obtain

$$\frac{\partial \bar{\omega}}{\partial t} + \mathbf{u} \cdot \nabla \bar{\omega} = -D(\beta(t)\psi + \alpha(t) + \bar{\omega}), \quad (154)$$

with  $\bar{\omega} = -\alpha(t)$  on the domain boundary. The Lagrange multipliers  $\beta(t)$  and  $\alpha(t)$  evolve so as to satisfy the constraints. Substituting Eq. (153) in Eqs. (149) and (150), we obtain the algebraic equations

$$\langle \psi^2 \rangle \beta(t) + \langle \psi \rangle \alpha(t) = -2E, \quad (155)$$

$$\langle \psi \rangle \beta(t) + \alpha(t) = -\Gamma. \quad (156)$$

Substituting  $\bar{\omega}$  taken from Eq. (153) in Eq. (148) and using the constraints (149)-(150), we easily obtain

$$\dot{S} = \int \frac{X^2}{D} d\mathbf{r}, \quad (157)$$

so that  $\dot{S} \geq 0$  provided that  $D$  is positive. On the other hand  $\dot{S} = 0$  iff  $X = 0$  leading to the condition of equilibrium (53). From Lyapunov's direct method, we conclude that these relaxation equations tend to a maximum of entropy (or a minimum of enstrophy) at fixed energy and circulation.

*Alternative relaxation equation:* writing the r.h.s. of Eq. (147) in the form of the divergence of a current in order to conserve the circulation, and using a MEPP, we obtain a relaxation of the form [34]:

$$\frac{\partial \bar{\omega}}{\partial t} + \mathbf{u} \cdot \nabla \bar{\omega} = \nabla \cdot [D (\nabla \bar{\omega} + \beta(t) \nabla \psi)], \quad (158)$$

$$\beta(t) = \frac{-\int D \nabla \bar{\omega} \cdot \nabla \psi d\mathbf{r}}{\int D (\nabla \psi)^2 d\mathbf{r}}. \quad (159)$$

The boundary conditions are  $(\nabla \bar{\omega} + \beta(t) \nabla \psi) \cdot \mathbf{n} = 0$  on the domain boundary. This relaxation equation satisfies the same general properties as Eq. (154). If we assume that  $D$  is constant, the foregoing equation can be rewritten

$$\frac{\partial \bar{\omega}}{\partial t} + \mathbf{u} \cdot \nabla \bar{\omega} = D (\Delta \bar{\omega} - \beta(t) \bar{\omega}), \quad (160)$$

$$\beta(t) = -\frac{\int \bar{\omega}^2 d\mathbf{r}}{2E} = \frac{S(t)}{E}, \quad (161)$$

where we have used an integration by parts to obtain the second term of Eq. (161).

*Remark:* Since these relaxation equations solve (11), they can also be used as a numerical algorithm to construct nonlinearly dynamically stable stationary solutions of the 2D Euler equations characterized by a linear  $\omega - \psi$  relationship (see Secs. 2 and 3) independently of the statistical mechanics interpretation.

## References

1. G.R. Flierl, *Annu. Rev. Fluid Mech.* **19**, 493 (1987)
2. P.S. Marcus, *Annu. Rev. Astron. Astrophys.* **31**, 523 (1993)
3. J.C. McWilliams, *J. Fluid Mech.* **146**, 21 (1984)
4. P. Tabeling, *Phys. Rep.* **362**, 1 (2002)
5. H.J.H. Clercx, G.J.F. van Heijst, *App. Mech. Rev.* **62**, 020802 (2009)
6. N.P. Fofonoff, *J. Mar. Res.* **13**, 254 (1954)
7. G. Veronis, *Deep-Sea Res.* **13**, 31 (1966)
8. A. Griffa, R. Salmon, *J. Mar. Res.* **49**, 53 (1989)
9. P.F. Cummins, *J. Mar. Res.* **50**, 545 (1992)
10. J. Wang, G.K. Vallis, *J. Mar. Res.* **52**, 83 (1994)
11. E. Kazantsev, J. Sommeria, J. Verron, *J. Phys. Oceano.* **28**, 1017 (1998)
12. P.P. Niiler, *Deep-Sea Res.* **13**, 597 (1966)
13. J. Marshall, G. Nurser, *J. Phys. Oceano.* **16**, 1799 (1986)
14. F.P. Bretherton, D.B. Haidvogel, *J. Fluid. Mech.* **78**, 129 (1976)
15. G.K. Batchelor, *Phys. Fluid. Suppl.* **12**, 233 (1969)
16. W. Matthaeus, D. Montgomery, *Ann. N.Y. Acad. Sci.* **357**, 203 (1980)
17. C.E. Leith, *Phys. Fluid.* **27**, 1388 (1984)
18. R. Kraichnan, *Phys. Fluid.* **10**, 1417 (1967)
19. R. Kraichnan, *J. Fluid. Mech.* **67**, 155 (1975)
20. R. Salmon, G. Holloway, M.C. Hendershott, *J. Fluid. Mech.* **75**, 691 (1976)
21. L. Onsager, *Nuovo Cimento Suppl.* **6**, 279 (1949)
22. G. Joyce, D. Montgomery, *J. Plasma Phys.* **10**, 107 (1973)
23. T.S. Lundgren, Y.B. Pointin, *J. Stat. Phys.* **17**, 323 (1977)
24. J. Miller, *Phys. Rev. Lett.* **65**, 2137 (1990)
25. R. Robert, J. Sommeria, *J. Fluid. Mech.* **229**, 291 (1991)
26. P.H. Chavanis, J. Sommeria, *J. Fluid. Mech.* **314**, 267 (1996)
27. H. Brands, P.H. Chavanis, R. Pasmanter, J. Sommeria, *Phys. Fluids* **11**, 3465 (1999)
28. P.H. Chavanis, J. Sommeria, *J. Fluid. Mech.* **356**, 259 (1998)
29. R. Ellis, K. Haven, B. Turkington, *Nonlin.* **15**, 239 (2002)
30. P.H. Chavanis, *Physica D* **200**, 257 (2005)
31. P.H. Chavanis, *Physica D* **237**, 1998 (2008)
32. F. Bouchet, *Physica D* **237**, 1978 (2008)
33. R. Ellis, K. Haven, B. Turkington, *J. Stat. Phys.* **101**, 999 (2000)
34. P.H. Chavanis, *Eur. Phys. J. B* **70**, 73 (2009).
35. R. Monchaux, F. Ravelet, B. Dubrulle, A. Chiffaudel, F. Daviaud, *Phys. Rev. Lett.* **96**, 124502 (2006)
36. R. Monchaux, P.P. Cortet, P.H. Chavanis, A. Chiffaudel, F. Daviaud, P. Diribarne, B. Dubrulle, *Phys. Rev. Lett.* **101**, 174502 (2008)
37. A. Naso, R. Monchaux, P.H. Chavanis, B. Dubrulle, [arXiv:0912.5102].
38. A. Renyi, *Probability theory*. North-Holland Publ. Company, Amsterdam (1970)
39. T.D. Frank, *Nonlinear Fokker-Planck Equations: Fundamentals and Applications* (Springer-Verlag, 2005)
40. A. Venaille, F. Bouchet, *Phys. Rev. Lett.* **102**, 104501 (2009)
41. G.H. Keetels, H.J.H. Clercx, G.J.F. van Heijst, *Physica D* **238**, 1129 (2009)
42. J.B. Taylor, M. Borchardt, P. Helander, *Phys. Rev. Lett.* **102**, 124505 (2009)
43. H.J.H. Clercx, S.R. Maassen, G.J.F. van Heijst, *Phys. Rev. Lett.* **80**, 5129 (1998)
44. A. Naso, P.H. Chavanis, B. Dubrulle, in preparation.
45. F. Bouchet, E. Simonnet, *Phys. Rev. Lett.* **102**, 094504 (2009)
46. S. Dubinkina, J. Frank, *J. Comput. Phys.* **227**, 1286 (2007)
47. P.H. Chavanis, *AIP Conf. Proc.* **970**, 39 (2008)
48. P.H. Chavanis, A. Naso, B. Dubrulle, [arXiv:0912.5096].
49. J. Sommeria, *J. Fluid. Mech.* **170**, 139 (1986)
50. H. Risken, *The Fokker-Planck equation* (Springer, 1989)
51. R. Benzi, *Phys. Rev. Lett.* **95**, 024502 (2005)
52. P.H. Chavanis, [arXiv:1002.0291]
53. A. Campa, P.H. Chavanis, [arXiv:1003.2378]
54. R. Robert, J. Sommeria, *PRL* **69** (1992) 2776.